Assessment of the environmental sustainability of solvent-less fatty acid ketonization to bio-based ketones for wax emulsion applications†

Bert Boekaerts, [a] Margot Vandeputte,[a] Kranti Navaré, [b,c] Joost Van Aelst,[a] Karel Van Acker, [b,d] Jan Cocquyt,[e] Chris Van Caneyt,[e] Peter Van Puyvelde[f] and Bert F. Sels *[a]

The environmental and economic challenges currently faced by the wax market may be addressed by the use of sustainable bio-based alternatives. Hereto, ketonization of vegetable oils and animal fats is a potential clean reaction route towards ketone bio-waxes. In the presence of a heterogeneous TiO_2 catalyst, palm fatty acid distillate (PFAD) and other commercial feedstock are selectively coupled to bio-waxes in a solvent-less liquid phase ketonization process. The resulting ketone bio-waxes show similar, if not better water repellence properties than the current benchmark paraffin waxes when tested as hydrophobization agents in aqueous wax emulsions for wood composite materials. Despite the efficient utilization of biomass carbon in accord with the prescribed Green Chemistry principles in the catalytic ketonization reaction, sustainable end products are not always guaranteed. Depending on the substrate and system scenario, the comparative life cycle assessment (LCA) shows significantly lower or higher carbon footprints in comparison to fossil paraffin. Cultivation of biomass feedstock, catalyst production and the end-of-life phase are identified as the three major hotspots in the life cycle, while the gate-to-gate impact of the proposed ketonization process design itself is rather limited. Advice is formulated to considerably improve LCA of ketone bio-waxes, achieving sustainable waxy products with appreciably lower CO_2 footprints than the fossil paraffin waxes.

1. Introduction

Current global challenges, related to our fossil-based economy, require efficient, renewable and sustainable bio-based processes, energy sources and chemicals to mitigate the harmful impact on climate, environment, and socio-economic and geopolitical stability.[1,2] Paraffin waxes are an archetypal example of petrochemicals which are currently used in a wide variety of applications such as candles, packaging, coatings, cosmetics, emulsions, rubbers, phase change materials, lubricants, *etc*. The market of these long-chain alkanes (mainly C_{20} to C_{40} range), derived from solvent dewaxing processing during lubricant base oil synthesis in the petroleum refinery, is encountering environmental and economic challenges.[3,4] Despite the consumer demand increase, wax production has decreased due to refinery plant shutdowns and increased interest for (hydro)cracking and hydro-isomerization towards fuels and lubricant base oils, resulting in short term price increases and potential future scarcity.[5,6] Alternative synthetic wax technologies exist, such as Fischer–Tropsch (FT) waxes from syngas and polyalphaolefines (PAO) from alkene monomers. However, they suffer from several drawbacks such as poor product selectivity, use of harmful catalysts, feedstock that are mainly derived from coal, natural gas and petroleum, and final products that are not price-competitive with the current waxes.[7–10] Even though biological animal (beeswax, lanolin, tallow, *etc*.) and vegetable waxes (candelilla, carnauba, jojoba, *etc*.) are used in many applications today, their restricted availability limits their potential to replace a substantial part of the current global wax market. This potential scarcity and expensiveness of waxes on the one hand, and the need for more sus-

[a]*Department of Microbial and Molecular Systems (M²S), Centre for Sustainable Catalysis and Engineering (CSCE), KU Leuven, Celestijnenlaan 200F, 3001 Leuven, Belgium*

[b]*Department of Materials Engineering, KU Leuven, Kasteelpark Arenberg 44 box 2450, BE-3001 Leuven, Belgium*

[c]*Unit Sustainable Materials, VITO, Boeretang 200, 2400 Mol, Belgium*

[d]*Center for Economics and Corporate Sustainability (CEDON), KU Leuven, Warmoesberg 26, BE-1000 Brussels, Belgium*

[e]*GOVI NV, Landegemstraat 8, 9031 Drongen, Belgium*

[f]*Department of Chemical Engineering, KU Leuven, 200F, B-3001 Heverlee, Belgium.*

E-mail: bert.sels@kuleuven.be

tainable and renewable bio-based chemicals on the other are strong incentives to seek for alternative competitive technologies and feedstocks.

We and others have recently reviewed the ketonization of carboxylic acids,[11,12] a potential clean biomass valorisation step as it does not require any solvents, additives or other toxic or harmful components. This C–C coupling, its roots originating from commercial production of acetone in the 19th century,[13] transforms two carboxylic acid molecules into an internal ketone, water and carbon dioxide, according to the general reaction equation (eqn (1)):

$$\mathrm{RCOOH} + \mathrm{R'COOH} \rightarrow \mathrm{RCOR'} + \mathrm{H_2O} + \mathrm{CO_2}. \quad (1)$$

Recent ketonization studies have focussed largely on the gas-phase coupling of lignocellulose derived carboxylic acids, present in pyrolysis bio-oil, producing moderate length C_3–C_7 ketones from C_2–C_4 acids.[12,14–16] These compounds are mainly proposed as precursors for bio-based fuels, requiring consecutive hydrodeoxygenation steps.[17,18] Given the sheer volume of liquid hydrocarbon fuels produced and consumed currently, it would require an unrealistic shift in the use of (lignocellulose) biomass to replace them.[19] Surprisingly, vegetable oils and animal fats, predominantly containing long-chain C_{12} to C_{18} fatty acids in their triglyceride biomass, have received far less attention as feedstock for ketonization. In our opinion, their large scale availability, limited chemical functionality and specific carbon chain length should make them suitable substrates for the envisioned C–C coupling. Following this route, renewable waxes can be produced without utilization of solvent. These ketones with 23 to 35 carbon atoms can potentially replace classic paraffin waxes in certain applications. In this context, the use of (non-food) oleochemical biomass waste streams or by-products, which are currently not valorised and destined for landfill or incineration, are particularly interesting to reduce the overall carbon footprint of the wax market.[20,21]

A limited amount of relevant fatty acid ketonization work has been published. For instance, high lauric acid conversion (96%) and C_{23} ketone selectivity (98%) were achieved in a gas-phase fixed bed process over MgO catalyst at 400 °C.[22] More recently, the impact of the degree of substrate unsaturation was studied using C_{18} fatty acids (stearic, oleic and linoleic) in a fixed bed gas-phase reactor at 380 °C and atmospheric pressure using a TiO_2 catalyst.[23] While no significant differences in overall conversion rate were observed, it was shown that the ketonization selectivity to C_{35} ketones decreased from 89 to 75% with increasing unsaturation at full conversion. Side products mainly included C_{16} olefins and C_{19} methyl ketones, as well as smaller amounts of hydrocarbons ($<C_{15}$) and C_{20} to C_{30} ketones as a result of decomposition pathways *via* initial McLafferty rearrangements of the fatty ketones. Using palm oil fatty acids, the ketone yield dropped further from 75 to 50% after 40 hours on stream. To mitigate this performance loss, a "hydrogenative hydrolysis" step was added, combining hydrogenation and hydrolysis of the unsaturated triglycerides before ketonization using a 5% Pt/C catalyst under 15 bar hydrogen pressure. The pre-saturated fatty acid mixture yielded a 91% total ketone mixture with higher selectivity and time-on-stream stability. In another study, refined seed oil of *Cuphea* sp. was used in the cross-ketonization reaction with acetic acid to 2-undecanone on a $Fe_{0.5}Ce_{0.2}Al_{0.3}O_x$ catalyst at 400 °C.[24] In this case, ketonization and transesterification between both substrates resulted in water formation and by extent (intermediate) free fatty acids could be generated from the *in situ* hydrolysis of the triglyceride. Post-reaction characterization of the spent catalyst revealed that the glycerol by-product was lost *via* cracking side reactions under the ketonization conditions. Similarly, glycerol degradation was found as the main source for the presence of CO, CO_2, acrolein and light hydrocarbons during the ketonization of palm oil in a batch reactor at 420 °C.[25] Full palm oil conversion was reached after two hours with a MgO–Al_2O_3 catalyst, resulting in 18, 22 and 55% yield of gaseous products, liquid hydrocarbons and ketones, respectively. The impact of specific substrate type (*e.g.*, sunflower oil, methyl stearate and oleic acid) was also investigated by isotopic labelling experiments during ZrO_2 catalysed ketonization.[26] Multiple side reactions such as cracking, Diels–Alder coupling, deoxygenation and aromatization were identified. Analysis of the ^{13}C isotope distribution in the gaseous effluent products suggested the occurrence of free radical mechanisms, with glycerol splitting into methanol and C_2 fragments under the ketonization conditions as an important initiator when directly using triglyceride substrates. In addition, C–C bond scission of the ketones can lead to radical chain reactions of the formed alkyl chains to form other numerous pyrolysis products.

A number of patent applications have recently been published on fatty acid/triglyceride ketonization using (mixed) metal oxide catalysts.[27–34] These ketonization processes are followed by commercially available hydrodeoxygenation and hydro-isomerisation steps to produce isomerised lubricant base oils. Besides reduction of CO_2 emissions, superior product properties such as absence of sulphur, nitrogen and aromatic compounds are mentioned to differentiate them from the current petroleum derived products. While paraffin is the desired end-product, alternative molecules have been synthesized from the fatty ketone intermediates in search of new applications. For instance, hydrogenation of coconut based fatty ketones to secondary fatty alcohols has been reported.[35] In a consecutive step these alcohols can be dehydrated to internal olefin intermediates, which are ultimately sulfonated to long internal olefin sulfonates, which are useful in the surfactant industry.[36]

Departing from the reasoning that their feedstock has sequestrated CO_2 during plant growth, bio-based products seem to have great potential as sustainable alternatives because they stock carbon during their use phase and reemit the same amount at their end-of-life phase. For this carbon cycle, it is common to assume that the intrinsic character of bio-based products is far more carbon neutral than that of their fossil counterparts. As a result, plant-based products may often benefit from a green and environmentally friendly repu-

tation. However, a critical attitude is at place here as this argument of carbon neutrality is widely debated.[37–39] Looking at sustainability from a holistic perspective, the cultivation of biomass to drive a bio-based economy exposes a number of potential challenges such as land use change (emissions), biodiversity loss, soil degradation, competition for food, economic viability, *etc*. In this context, a life cycle assessment (LCA) was recently published encompassing 6 different process scenarios for lignocellulose pyrolysis bio-oil upgrading to liquid hydrocarbon fuels.[40] For the ketonization step, an electricity cost of 0.25 kW h kg^{-1} of light oxygenates was calculated using 5 wt% $Ru/TiO_2/C$ catalyst, assuming 46% ketone yield at 400 °C based on previous experimental work by Pham *et al.*[41] For both scenarios involving a ketonization reaction, it was shown that the global warming potential (GWP) attributed to ketonization and/or esterification was the lowest. While very limited information can be extracted from the above work for ketonization, no detailed process design and environmental sustainability analysis was performed on the C–C coupling reaction separately.

As shown in this introduction, important advances have been made in the understanding of catalytic ketonization of carboxylic acids,[12,14,15,42] but many prominent questions and challenges remain unanswered in order for this technology to really compete with and substitute a part of the current petroleum derived waxes. To the best of our knowledge, no LCA study has been performed on the on-purpose ketonization of carboxylic acids specifically, and especially not regarding the use of fatty acids in the liquid phase. This may be attributed to the lack of information about the techno-economic aspects of a reliable, integrated process design, despite its importance for development and evaluation of application potential. Related to the latter, characterization of the physicochemical properties of the final ketone products and application testing in current wax applications are important subjects that have not received adequate attention yet. In fact, if these molecules can be used as end products in existing and future applications, any further downstream processing technologies such as hydrodeoxygenation can be omitted. In this case, both the economic and environmental cost will be lower and will thus result in stronger cases for the ketonization processes in future biorefineries. To address these outlined information gaps surrounding fatty acid ketonization for bio-wax production, the major objectives of this study are threefold. First, industrially relevant ketonization conditions will be determined based on lab scale experimental screening work using a commercial fatty acid feedstock (palm fatty acid distillate – PFAD) and commercially available TiO_2 catalysts in a liquid phase solvent-free reaction. This will allow the design of a large scale industrial process design with full mass and energy balances. Secondly, the bio-wax products will be characterized extensively, and their application potential will be tested in typical wax emulsions for use in hydrophobic coatings (Fig. 1). Finally, the results of the first two objectives will result in a Green Chemistry and comparative LCA analysis to evaluate the environmental sustainability of the bio-based ketones in comparison to classic paraffin wax for various impact categories, identifying important CO_2 footprint hurdles.

2. Experimental

2.1. Chemicals & materials

2.1.1. Substrates. Lauric acid (98%) and myristic acid (98%) were purchased from Sigma Aldrich. Palmitic acid (98%) and stearic acid (97%) were purchased from Acros Organics. Oleic acid (90% tech.) was purchased from Fisher Scientific. Commercial palm fatty acid distillate (PFAD) was provided by Cargill (Agri-pure AP-135). Sonac animal fatty acids were provided by Sonac. Distilled topped coconut fatty acids were provided by Wilmar (Wilfarin DC-1288). Topped palm kernel fatty acids were provided by KLK Oleo (Palmera B1220).

2.1.2. Products. Laurone (12-tricosanone, 95%), myristone (14-heptacosanone, 95%), palmitone (16-hentriacontanone, 95%) and stearone (18-pentatriacontanone, 95%) were purchased from TCI Europe. Hydrogenated C_{36} fatty acid dimer mixture was provided by Oleon. Fully refined paraffin wax was

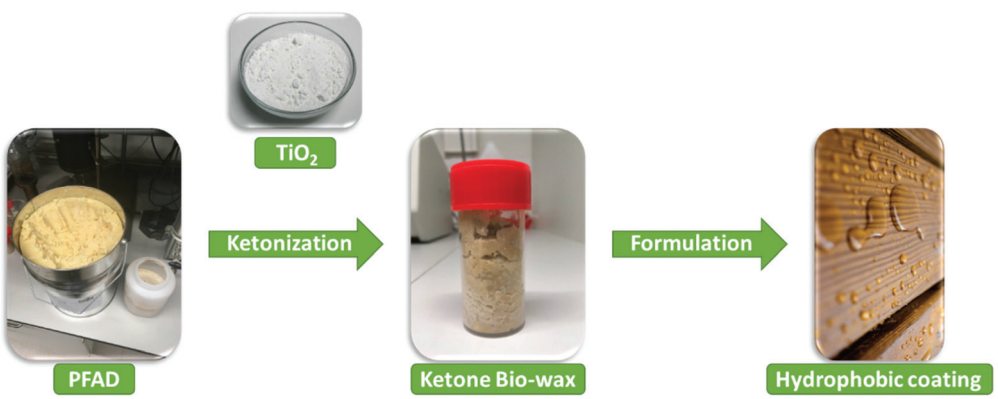

Fig. 1 Ketonization of palm fatty acid distillate (PFAD) with a TiO_2 heterogeneous catalyst as a valorisation strategy to produce bio-based ketones for wax applications such as hydrophobization.

provided by Sasol. Dotriacontane (97%) was purchased from Sigma Aldrich.

2.1.3. Catalysts. Commercial TiO_2 catalysts were provided by Kronos (KRONOKat 7500) and Venator (Hombikat M211). The commercial PRICAT Ni 52/35 hydrogenation catalyst (50% Ni on Kieselguhr support, 3 mm pellets) was purchased from Johnson Matthey.

2.1.4. Others. Eicosane (99%) and chloroform (HPLC grade) were purchased from Acros Organics. *N*-Methyl-*N*-(trimethylsilyl)trifluoroacetamide (MSTFA, 98.5%) and tetrahydrofuran (99%) were purchased from Sigma Aldrich.

2.2. Characterization

2.2.1. X-ray diffraction. PXRD analysis of the catalyst was carried out on a high-throughput STOE Stadi P Combi diffractometer with an image plate position sensitive detector (IP-PSD) for 2θ = 5–60° and a scan of maximum 1200 s. The measurements were performed in transmission mode using CuKα1 radiation (λ = 1.54056 Å) selected by a Ge (111) monochromator.

2.2.2. Scanning electron microscopy. First, the catalyst sample was coated with a gold layer using a JEOL JSC-1300 sputter instrument. Afterwards, images were taken with a JEOL JSM-6010 JV microscope while applying an accelerating voltage of 10 kV.

2.2.3. Nitrogen physisorption. The measurements were carried out with a Micromeritics Tristar II 3020 instrument at −196 °C. First, catalyst samples (50–100 mg) were degassed for 5 hours in a continuous nitrogen flow at 300 °C before measurement. The surface area was determined according to BET theory.

2.2.4. Temperature-programmed desorption. NH_3–TPD measurements were carried out in a custom flow setup with a Pfeiffer Omnistar quadrupole mass spectrometer to analyse the composition of desorbed gasses (signal m/z = 16 was used for NH_3). First 100 mg of catalyst sample was pre-treated in He flow at 400 °C for 1 hour with a heating rate of 5 °C min^{-1} starting from room temperature. Next, the sample was cooled off and adsorption of ammonia was conducted at 150 °C for 30 minutes after which the sample was flushed with He for an additional 30 minutes. Finally, the sample was heated to 800 °C with a rate of 10 °C min^{-1} in helium during the desorption measurements. For CO_2–TPD measurements, the same setup was used with detection of the CO_2 signal by MS (m/z = 44). While the initial pre-treatment was the same as the ammonia measurements, the adsorption temperature was lowered to 50 °C. All other steps remained unchanged. Deconvolution of data was performed with OriginPro software.

2.2.5. Pyridine FT-IR spectroscopy. After preparation of self-supporting wafers, the catalysts were pre-treated at 400 °C and 1 mbar vacuum for 1 h. To determine Lewis (L) and Brønsted (B) acid sites, the samples were saturated with pyridine (25 mbar) at 50 °C. The samples were degassed at 150, 250 and 350 °C before collecting data at 150 °C. The analysis was carried out on a Nicolet 6700 spectrometer with DTGS detector (256 scans per spectrum, 2 cm^{-1} resolution). An extinction coefficients value of 1.63 cm μmol^{-1} was used for Lewis acid sites.[43]

2.2.6. Thermogravimetric analysis. To determine the amount of water and organic coke formation *via* (relative) weight loss, TGA analysis of fresh and spent ketonization catalyst was performed on a TA Instruments TGA Q500 machine. Starting at room temperature, the catalyst sample (10 mg) was heated to 700 °C under O_2 flow with a heating rate of 5 °C min^{-1} starting from room temperature. To investigate the thermal and oxidative stability of the bio-wax products, a similar TGA procedure was followed.

2.2.7. Differential scanning calorimetry. DSC experiments were performed on a TA Instruments DSC Q2000 instrument. Typically, 5–8 mg of sample was precisely weighed in aluminium pans and closed off with non-hermetic lids. After equilibration at 100–120 °C for 5 minutes, temperature cycling was done between −40 and 120 °C or 20–100 °C for 2 cycles with a heating rate of 5 °C min^{-1} under constant N_2 flow (50 ml min^{-1}).

2.2.8. Viscosity measurement. A Physica MCR 501 rotational rheometer (Anton Paar) was used to determine the viscosity of fatty acid substrates and ketone wax products. A titanium cone-plate CP50-1 (50 mm diameter, 1° cone angle) geometry system was used. Heating was established *via* a Peltier element and measurements were performed at 100 °C. The shear rate was increased from 0.1 to 100 Hz over a total of 160 seconds with data collection every 10 seconds.

2.3. Ketonization and hydrogenation reactions

2.3.1. Ketonization reaction procedure. In a typical experiment, 40 g of fatty acid substrate is loaded into a 100 ml Parr (semi-) batch reactor together with the desired amount of TiO_2 catalyst. First, the reaction mixture is melted by heating to 100 °C before flushing out the air by adding 10 bar of inert N_2 pressure and stirring at 600 rpm for 90 seconds, after which the head space is evacuated. This flushing procedure is repeated 3 times to ensure an inert reaction atmosphere during reaction. Afterwards, starting from atmospheric pressure and 100 °C for a typical batch experiment, the temperature is increased to the desired reaction temperature with a heating rate of 8 °C min^{-1}. For semi-batch experiments, a continuous N_2-flow (1–60 ml min^{-1}), which is controlled by BRIGHT series modules by Bronkhorst, is passed through the liquid reaction medium *via* a gas inlet tube connected to the mechanical stirrer. The head space outlet gas is passed through a condenser system, which is maintained at 5 °C, in such a way to avoid any substrate or product loss besides N_2, CO_2 or other gasses. A constant reaction pressure is provided in these semi-batch experiments and controlled by back pressure regulators. After the desired reaction time has expired, the reactor is cooled to 95 °C with an ice bath and depressurized before opening.

2.3.2. Hydrogenation reaction procedure. For hydrogenation of unsaturated fatty acids before ketonization, 40 g of substrate was loaded into the 100 ml Parr batch reactor. A cata-

lyst basket, attached to the mechanical stirrer, was used for the hydrogenation catalyst (PRICAT Ni 52/35), which was used in pellet form (3 g). The flushing procedure was identical to that of the ketonization reaction. After flushing, a H_2 pressure of 30 bar was applied at 100 °C and the temperature was raised to 210 °C for 8 hours. After hydrogenation, the reactor was cooled with an ice bath and the hydrogenation catalyst was simply removed by detaching the catalyst basket from the mechanical stirrer.

2.3.3. Product analysis. Eicosane (2 g) is added as internal standard and the reactor content is stirred for an additional 10 minutes at 95 °C for homogenization purposes. Next, 0.5 g of sample is dissolved in 5 ml chloroform, after which it is centrifuged at 3500 rpm for 15 minutes to ensure full catalyst separation. Afterwards, 1 ml of supernatant is derivatised *via* trimethylsilylation using an excess of MSTFA and heating at 60 °C for 30 minutes to guarantee full conversion of unreacted fatty acid substrate. Gas chromatography (GC) was performed using an Agilent 6890 instrument equipped with an Agilent HP-5 column (30 m, 0.32 mm internal diameter, 0.25 μm film thickness) and a flame ionization detector (FID at 320 °C). The injection volume was 1 μl and a split ratio of 10 : 1 was used with N_2 as carrier gas. Injection and initial oven temperatures were 300 and 60 °C, respectively. The oven temperature was then increased to 190 °C with a heating ramp of 10 °C min^{-1}, from 190 to 200 at 1 °C min^{-1}, from 200 to final 310 °C at 5 °C min^{-1}, which was held for an additional 15 minutes. Quantification was performed *via* calibration curves obtained using the eicosane standard and purchased pure analytical grade fatty acids and ketones. Additional identification of unknown or commercially unavailable compounds was carried out *via* gas chromatography–mass spectrometry (GC–MS) using an Agilent 5973 instrument equipped with a HP-5 ms column (25 m, 0.25 mm internal diameter, 0.25 μm film thickness), for which the same GC–FID temperature program was used. Analysis of the head space gas composition after batch reaction was carried out on a dual channel Interscience Trace GC instrument equipped with a RTX-1 column and FID detector, and a Hayesep Q column with thermal conductivity detector (TCD). The distribution of the molecular weight of the solid wax compounds was investigated using gel permeation chromatography – size exclusion (GPC–SEC). Samples (20 mg) were solubilized in THF (4 ml) and afterwards filtered with a 0.2 μm PTFE membrane to remove any particulate matter. GPC–SEC analysis was performed at 40 °C on a Waters E2695 Separation Module instrument equipped with a PL-Gel 3 μm Mixed-E column, using THF as solvent with a flow of 1 ml min^{-1}. A Waters 2414 refractive index (RI) detector was used. Proton nuclear magnetic resonance (^{1}H-NMR) analysis was performed in the liquid phase using a Bruker Avance III HD 400 MHz instrument with autosampler. Approximately 20 mg of crude wax sample was dissolved in 0.5 ml deuterated chloroform with TMS and filtered with a 0.2 μm PTFE membrane before transferring to an NMR tube. The spectra were acquired at 25 °C, using a pulse angle of 30°. The chemical shifts (ppm) are referenced to tetramethylsilane.

2.3.4. Catalyst separation. To test the catalyst stability, the catalyst was separated from the liquid reaction product *via* a heated centrifugation step at 100 °C and 5000 rpm for 30 minutes to ensure full precipitation of the catalyst.

2.4. Aqueous wax emulsion application testing

For detailed procedures regarding the application testing, the reader is referred to an earlier pending patent application which includes the general preparation procedure of the aqueous phase wax emulsions, particle board testing and application evaluation for hydrophobization.[44]

2.5. Green Chemistry

The Green Chemistry concept focuses on waste prevention by evaluating chemical reactions and their corresponding processes on the basis of 12 fundamental principles and 7 measuring instruments.[45] One of the first and most telling Green Chemistry measures is the *E*-factor, which expresses the amount of waste (kg) produced per kg of desired product. In this case, total waste means all waste including non-converted reactants or auxiliaries, undesired reaction products and losses due to solvent recovery and other post-treatments. The only common exception to this rule is water, which is often not taken into account as waste because its inclusion leads to peculiarly high *E*-factors making representative comparisons difficult. Secondly, the atom economy/efficiency is defined as the ratio of the molecular weight of the desired product over the molecular weight of the reactants. Since molecular weights are used for its calculation, atom economy is a theoretical measure which can be used to assess the initial acceptability of a chemical reaction or process. The effective mass yield (EMY) describes how much kg of desired product can be obtained per unit of mass of "non-benign" reagents. A fourth measure is known as the mass intensity (MI), which shows the total amount of mass required to produce a unit of product on a wt/wt basis. The following relation between the *E*-factor and the mass intensity of a reaction holds true: MI = *E*-factor + 1. The ideal *E*-factor being zero logically leads to an ideal MI of 1. In contrast to the previous two measuring instruments, the mass intensity takes into account all types of reactants, solvents and auxiliaries as well as the actual reaction yield. As a fifth measure, the mass productivity is simply the reciprocal of the mass intensity and equals the effective mass yield in case there is no solvent waste generated and all reagents are considered non-benign. Given the increased awareness of the fragility of our carbon cycle and the impact of its disruption on the current wellbeing of our planet and its societies, a sixth measure covers information about the carbon balance of a chemical reaction or process. The carbon efficiency is defined as the percentual ratio of the effective amount of carbon in a product over the total amount of carbon in the reagents. By taking into account both the reaction yield and stoichiometry, this measure indicates how sparingly carbon is used. The last measure is known as the reaction mass efficiency (RME), which reveals the 'greenness' of a reaction because, in addition to the reaction stoichiometry and yield, also the atom

economy is taken into account. The RME reflects in mass percentage how much of the reagents ends up in the final product and equals the effective mass yield when all reagents are considered non-benign.

2.6. Life cycle assessment

2.6.1. Goal. The goal of the comparative life cycle assessment is to quantify the overall environmental impact of the bio-based ketone wax (LCA_b) relative to that of the benchmark petroleum-based wax or paraffin wax (LCA_p). The comparative LCA in this work is conducted in line with the standardised methodological framework existing of two International Standards: ISO 14040 and ISO 14044. ISO 14040 [46] describes the principles and framework for life cycle assessment, while ISO 14044 [47] specifies requirements and provides guidelines for life cycle assessment. When conducting a LCA, it is important to validate the influence of the assumptions made and data used. Therefore, uncertainty and sensitivity analyses are included in order to reflect on the assumptions and to identify the key parameters influencing the resulting impacts.

2.6.2. Functional unit. Since the bio-wax ketones are tested in aqueous wax emulsions for hydrophobization of wooden composite materials, the functional unit (FU) has been defined as 1 kg of wax (fatty acid or petroleum based) ready to use in a wax emulsion product. Therefore, the reference flow is 1 kg of ketone wax or paraffin wax. The wax emulsions will be applied as hydrophobic coatings on wood composite panels with a suspected lifetime of 20 years. With 1 kg of wax, it is possible to coat approximately 40 m^2 of wood surface with two layers. The European Union is taken as the location for both the production of the waxes and wax emulsions, as well as for the application, use and incineration of the wood coating product. The two LCA studies (LCA_b and LCA_p) are compared based on their reference flows.

2.6.3. Methodology. An attributional life cycle model is used which implicates that all the impacts directly related to the supply chain of the wax emulsions are taken into account.[48] As impact assessment methodology, ReCiPe 2016 v1.1 is used as it is one of the most recent and harmonized methodologies available for conducting a reliable life cycle impact assessment.[49] A cradle-to-grave approach is chosen as this tends to be the most reliable, comparable and representative system boundary possible. For the base case scenario, economic allocation based on market prices has been chosen as the global warming impact of a product increases with increasing economic value.[39] The following impact categories have been selected for investigation: climate change excluding biogenic carbon (kg CO_2 eq.), climate change including biogenic carbon (kg CO_2 eq.), freshwater consumption (m^3), freshwater eutrophication (kg P eq.), human toxicity, non-cancer (kg 1,4-DB eq.), photochemical ozone formation ecosystems (kg NO_x eq.), photochemical ozone formation human health (kg NO_x eq.), terrestrial acidification (kg SO_2 eq.) and terrestrial ecotoxicity (kg 1,4-DB eq.).

2.6.4. Datasets and detailed description. The GaBi dataset "Wax/Paraffins at refinery; from crude oil; production mix, at refinery; 38 MJ kg^{-1} net calorific value (en)" has been chosen for the benchmark LCA_p.[50] This dataset covers the whole supply chain going from well drilling for crude oil extraction over processing and refining until the finished product of paraffin wax, including all relevant transportation *via* pipelines and/or vessels. Further detailed description is provided in the ESI.†

For the production of refined palm oil, the aggregated Gabi process data set "MY Palm oil, refined; technology mix; production mix, at plant; refined (incl. LUC as fossil CO_2)" is used.[51] This dataset is representative for the country of Malaysia (MY). In this study, transport to Europe by cargo ship has been modelled and included. The used GaBi dataset on the production of refined palm oil is based on the latest literature and the overall data quality is classified as very good by Thinkstep's data quality indicators system. Substrate transport, the use of this dataset and accompanying assumptions of this study are described in detail in the ESI.†

The end-of-life (EoL) incineration has been modelled the same way for both assessments, using the GaBi thinkstep process dataset for the waste incineration process of polyethylene (PE), except for the definition of the carbon dioxide emissions. The CO_2 from paraffin incineration is defined as fossil, while the CO_2 from the bio-wax incineration is defined as biogenic. The incineration process of PE can be regarded as a reasonable model for the incineration of wax given the major similarity in chemical structure between PE (C_nH_{2n}), paraffin wax ($C_nH_{2n+2)}$ and ketone bio-wax ($C_nH_{2n}O$). However, the calorific value of PE (43.5 MJ kg^{-1}) and wax (38 MJ kg^{-1}) is not identical and hence the electricity and heat produced by incinerating the two would be different. This has been accounted for by updating the output electricity and heat in the database process of PE by converting it based on the difference in calorific value. The thermal energy (steam) output as well as the electricity output are recovered (given credit) within the process.

2.6.5. General assumptions and limitations. To ensure a correct and representative comparison between LCA_b and LCA_p it is important to mention the following general aspects and assumptions which are the same for both life cyles: time horizon (100 years), geographical boundary (European Union), cut-off rules (coverage of at least 95% of mass and energy of the input and output flows, and 98% of their environmental relevance (according to expert judgement)), natural gas (EU-28 2014) and electricity mix (EU 28), temporal period (LCA_p: 2008–2017 and LCA_b: 2019), impact assessment methodology (ReCiPe 2016 v1.1 – Hierarchist (H) perspective) and reference flow (1 kg of wax ready to use in a wax emulsion product). While the aim is to have the same technological representativeness, it must be noted that LCA_p is based on optimised and mature refining and purification technologies, while LCA_b is based on upscaled lab results. This is also the main limitation of this comparative LCA. Furthermore, since this is a comparative study, any minor steps which are identical for LCA_p and LCA_b will have no influence on the comparability of the results and will therefore not be included in the analysis. These

include final processing operations of the wax products such as packaging and transfer to clients.

3. Results and discussion

As discussed in the introduction, the current state-of-the-art does not suffice to accurately perform a critical and extensive LCA of this biomass conversion reaction. An exploratory experimental catalytic study of fatty acid ketonization is therefore first performed in this work to acquire the required reaction conditions and process parameters for high conversion rate and ketone selectivity. These data are necessary for the major purpose of this study, which is to perform the first ketonization LCA.

3.1. Substrate analysis & catalyst characterization

The fatty acid profile of commercial PFAD – a by-product of palm oil refining – is given in Table 1. Apart from saturated palmitic (C16:0) and unsaturated oleic acid (C18:1) as the main compounds, it contains smaller amounts of myristic (C14:0), stearic (C18:0) and linoleic acid (C18:2). The substrate is a yellow to light brown semi-solid at room temperature as a result of this composition, while above its melting point (40–45 °C) the substrate is a brown translucent liquid.

Amphoteric oxides such as ZrO_2, TiO_2 and CeO_2 are cited as preferred ketonization catalysts due to their high activity and selectivity. Although debated, surface Lewis acid–base pairs (coordinatively unsaturated Ti^{x+}–O^{y-} species) are the generally accepted active sites which catalyse the C–C coupling *via* a β-ketoacid mechanism.[52,53] Here, two commercially available TiO_2 materials (KRONOKat 7500 (KK7500) from Kronos and Hombikat M211 (HM211) from Venator) were selected as potential catalysts for the ketonization of PFAD. Table 2 summarizes the physicochemical properties of these materials as determined *via* various characterization techniques (see ESI Fig. S1–S7† for extensive analysis and details).

Both TiO_2 catalysts materials are high surface area anatase catalysts containing only Lewis acid–base sites (Ti^{x+}–O^{y-}). The Lewis acidity of these catalysts originates from coordinatively unsaturated Ti^{x+} ions on the surface, acting as electron acceptors due to the presence of unoccupied orbitals in their valence electron shell. While Ti atoms in the stoichiometric bulk phase are coordinated by six O atoms, exposed Ti atoms on the surface can be coordinated by only five O ligands. Similarly, exposed coordinatively unsaturated O^{y-} ions at the surface act as Lewis bases (electron donors). In the stoichiometric bulk phase, O atoms are coordinated by three Ti atoms, while exposed O atoms on the surface can be coordinated by only two Ti ligands. In this manner, neighbouring Ti^{x+}–O^{y-} active centres are responsible for fatty acid adsorption, activation and ultimately ketonization on the TiO_2 surface. The (relative) strength of these Lewis acid–base sites (Ti^{x+}–O^{y-}) depends on their bonding interaction with the adsorbing (probe) molecules, which is inherently determined by the geometrical and electronic environment of the surface and its surroundings. These are affected by several material parameters of the heterogeneous materials such as Ti–O bond distances, nature of crystallographic surfaces, presence of defects, steps, edges, terraces, degree of surface (de)hydroxylation, *etc.*[54–56] The KK7500 catalyst has a higher Lewis acid site density with stronger acid sites compared to HM211, while the latter material has a higher base site density and stronger basicity (leaving potential formation of carbonates from CO_2).

Table 1 Fatty acid distribution of palm fatty acid distillate (PFAD) substrate

Name	Chemical formula	Wt%
Myristic acid	C14:0	1.2
Palmitic acid	C16:0	48.3
Stearic acid	C18:0	4.2
Oleic acid	C18:1	38.1
Linoleic acid	C18:2	8.1

Table 2 Summary of characterization results of TiO_2 catalysts used in this work

Catalyst property	KK7500	HM211
Crystal phase	Anatase	Anatase
Primary crystallite size (nm)[a]	9.6	7.8
Band gap (eV)	3.3	3.3
BET surface area ($m^2\ g^{-1}$)	248	266
Lewis acidity (μmol g^{-1}) at 150 °C	540	324
Lewis acidity (μmol m^{-2}) at 150 °C	2.17	1.22
Lewis acidity (μmol m^{-2}) at 250 °C	1.29	0.86
Lewis acidity (μmol m^{-2}) at 350 °C	0.52	0.42
Brønsted acidity (μmol g^{-1}) at 150 °C	<1	<1
Total relative acidity[b] (%)	122	100
Total relative basicity[b] (%)	24	100

[a] Based on XRD. [b] Based on total integrated TPD signal area per surface area of catalyst.

3.2. Fatty acid ketonization

The first goal of these ketonization screening experiments is the achievement of high substrate conversion rate and product selectivity under industrially relevant solvent-free process conditions in the liquid phase. This is indispensable to obtain reliable and essential data to design a large scale ketonization process, and from there the technical analysis and resulting LCA. Extensive optimization and modification of the catalysts on a microscopic level are not the primary objectives here, and will be published elsewhere. The initial screening was carried out using pure stearic acid (SA) as model compound to obtain the stearone (18-pentatriacontanone) product (Table 3, entries 1–10). The experiments were conducted in a liquid phase batch reactor without any solvent or additive, operating at autogenous pressures (5–40 bar depending on conditions). The starting temperature was selected based on a survey of the relevant literature.[11] Given that 1 mole of water and carbon dioxide are formed as co-products for each mole of ketone during the ketonization reaction, the maximum theoretical mass yield for stearone at full conversion (X) is 89%.

Table 3 Screening of liquid phase SA and PFAD ketonization using KK7500 and Hombikat M211 TiO_2 catalysts. m_{feed} = 40 g; stirring rate = 600 rpm. For batch reactions, the final autogenous pressures are shown

Entry	Feed	Catalyst	Loading (wt%)	t (h)	Mode	P (bar)	N_2-Flow (ml min^{-1})	T (°C)	X (wt%)	S (%)
1	SA	KK7500	40	1	Batch	13	—	340	30	99
2	SA	KK7500	40	2.5	Batch	31	—	340	92	99
3	SA	HM211	40	1	Batch	11	—	340	15	100
4	SA	HM211	40	2.5	Batch	19	—	340	62	99
5	SA	KK7500	20	2.5	Batch	26	—	340	48	99
6	SA	KK7500	6.75	1	Batch	6.4	—	340	5	99
7	SA	KK7500	6.75	2.5	Batch	15	—	340	16	98
8	SA	KK7500	6.75	2.5	Semi-batch	5	5	340	33	99
9	SA	KK7500	6.75	2.5	Semi-batch	5	20	340	40	99
10	SA	KK7500	6.75	2.5	Semi-batch	5	50	340	41	99
11	PFAD	KK7500	20	3	Batch	4.6	—	300	3	78
12	PFAD	KK7500	20	3	Batch	8.2	—	320	14	79
13	PFAD	KK7500	20	3	Batch	31	—	340	44	77
14	PFAD	KK7500	20	3	Batch	39	—	350	79	76
15	PFAD	KK7500	6.75	3	Batch	16	—	340	13	76
16	PFAD	KK7500	10	6	Batch	41	—	350	99	76
17	PFAD	KK7500	10	6	Semi-batch	5	20	350	100	76
18	PFAD	KK7500	5	4	Semi-batch	5	20	350	87	77
19	PFAD	KK7500	5	4	Semi-batch	5	20	360	100	69
20	PFAD	KK7500	2.5	6	Semi-batch	5	5	350	58	74
21	PFAD	KK7500	5	6	Semi-batch	5	5	350	99	75

Therefore, the selectivity (S) is expressed relative to the theoretical maximum for any given conversion value in this work.

From Table 3, it can be observed that all reactions gave (near to) full selectivity to the C_{35} ketone product for both TiO_2 catalysts. In some instances, a trace amount (1–2 wt%) of heptadecane was obtained as a result of the direct deoxygenation side-reaction of stearic acid *via* decarboxylation. Furthermore, the more Lewis acidic KK7500 catalyst showed both higher initial (entry 1 *vs.* 3) and total overall conversion rate (entry 2 *vs.* 4) for reaction times of 1 and 2.5 hours, respectively. Different KK7500 loadings (m_{cat}/m_{feed}) showed a linear correlation with the overall conversion, corresponding to an average ketone productivity of 0.94 ± 0.02 $g_{ketone}\ g_{cat}^{-1}\ h^{-1}$. Because CO_2 and H_2O are formed at 340 °C, an increase of the autogenous pressure inside the batch reactor was observed over time (example given in Fig. S8†). Given the reported product inhibition due to competitive adsorption of the three reaction products in the case of short-chain (C_2–C_4) carboxylic acid ketonization,[57,58] a drop in the conversion rate was also expected for the *liquid* phase ketonization of long fatty acids with increasing conversion. Additionally, it has been recently stated that ketonization could be an equilibrium reaction, for which the reverse reaction rate increases for elevated CO_2 pressures.[59,60] To compensate for these potential activity losses, the most active catalyst was tested in the so-called semi-batch operation modus. This allows a continuous in-and-out flow of the gas phase, by purging N_2 through the liquid reaction medium at constant pressure *via* a gas inlet tube connected to the mechanical stirrer. At the reactor outlet, a condenser maintained at 5 °C prevents any liquid substrate or product loss, as they are sent back into the reaction medium. The results are shown in entries 8–10, revealing considerable improvement of the conversion rate upon utilization of such reactor purging. The conversion rate of SA almost tripled (compared to batch system), corresponding to a space time yield of 2.4 $g_{ketone}\ g_{cat}^{-1}\ h^{-1}$ (Fig. S9†). Purging (of CO_2 and H_2O) is thus important to shorten the reaction time and use the catalyst more efficiently. Until today, only the negative impact of water has been reported in a single pending patent application in the case of liquid phase fatty acid ketonization with a TiO_2 catalyst, but not the effect of CO_2. On the contrary, the particular example used pure CO_2 as carrier gas, with no mention on its potential inhibition of the conversion rate, as shown here.[34]

Next, the ketonization of the commercial PFAD substrate was investigated (Table 3, entries 11–21). Increasing the reaction temperature between 300–350 °C (entries 11–14) increases the conversion rate according to an exponential Arrhenius relationship, with an observed activation energy of 177 kJ mol^{-1} after assuming a zero order reaction (Fig. S10†). In this work, pure fatty acid substrate is used without any solvent or additive, and relevant ketonization literature typically shows a zero order dependence at high(er) substrate concentrations due to saturation of the active sites under these circumstances.[61–63] This apparent activation energy value is in line with other reported values of 185 kJ mol^{-1} for ketonization of acetic acid on Ru/TiO_2 [58] and 160 kJ mol^{-1} for palmitic acid using K_2O/TiO_2.[34] Clearly, the liquid phase ketonization of fatty acids benefits from a high reaction temperature, which is related to the favourable thermodynamics given its endothermic reaction enthalpy.[34] Despite a considerable level of unsaturation and some non-fatty acid impurities in the feedstock (compared to pure SA), a mixture containing 75 wt% of C_{27}–C_{35} ketones is formed at 350 °C at full conversion (see next paragraph for detailed product analysis). Increasing the ketonization temperature further to 360 °C resulted in lower ketonization selectivity (69%), mainly due to increased deoxygenation reactions. Therefore, 350 °C was chosen due to the desirable balance of high activity, selectivity and industrial applica-

bility. As a conclusion of these screening experiments, the following conditions were selected as starting point for the base case LCA: a 5 wt% catalyst loading, and a 6 hours ketonization reaction carried out in semi-batch mode at 350 °C. These industrially relevant conditions provide PFAD conversion and an overall ketone productivity of 2.5 $g_{ketone}\ g_{cat}^{-1}\ h^{-1}$ and 3.3 $g_{wax}\ g_{cat}^{-1}\ h^{-1}$ for the total solid bio-wax.

The catalyst stability was tested as it determines the amount of active material that must be taken into account during the ketonization process design and the derived LCA. Therefore, three consecutive runs were performed under the base case conditions without any additional treatment between the experiments (Fig. S11†). A 45% decline in catalytic activity was observed for the third run with KK7500. Post-reaction analysis of the catalyst *via* TGA and N_2-physisorption techniques indicate that the loss of catalytic activity is attributed to the loss of surface area (sintering) and the presence of carbon cokes on the active material (Fig. S11 and S12†).

3.3. Bio-wax product analysis

To perform an accurate LCA, a detailed and complete mass balance is required, which is shown in Table 4 after full PFAD conversion. The solid wax product mainly contains C_{27}–C_{35} ketones due to the occurrence of both homo- and cross-ketonization between the different PFAD fatty acids. As PFAD consists of 38% oleic acid (C18:1) and 8% linoleic acid (C18:2), a multitude of different unsaturated C_{33} and C_{35} ketones can be formed due to positional and geometric C=C bond isomerisation under the ketonization conditions.[64] Around 1% of C_{15}–C_{17} hydrocarbons were present, due to decarboxylation side reactions. Thus, 24% of the solid mass balance remained unknown after GC(–MS) analysis. Therefore, additional analysis *via* GPC and ^{1}H-NMR was performed to investigate the impact of the (poly)unsaturation in the feedstock on the ketonization selectivity (see ESI† for extensive analysis). Firstly, GPC analysis indicated that the remaining unknowns in the wax fraction can be linked to molecular weights in the range of fatty acid dimers and trimers (Fig. S13†). It is well known that these high boiling C_{36} and C_{54} side products can be formed thermally or catalytically from oleic and linoleic acid *via* oligomerisation reactions at the double bond at elevated temperature (250 °C and higher). Typically, the final product of dimerization is a mixture containing unsaturated linear, cyclic and aromatic dimers and trimers (Fig. S14†).[65] In fact, fatty acid dimers are commercial products that are currently used as building blocks for polymers and as ingredients in the cosmetics industry, for example in skin and hair products. Other applications include lubricants, surfactants, resins, fuels and coatings. Their presence in the crude PFAD bio-wax product was further confirmed *via* ^{1}H-NMR (Fig. S15 and S16†), showing characteristic signals for the presence of unsaturated aromatic, cyclic and linear non-fatty acid carboxylic acids.[66] To further validate these findings, the original PFAD feedstock was subjected to a hydrogenation reaction prior to the ketonization in a separate experiment (ESI†). Ketonization of this (nearly) fully hydrogenated (~97% saturated fatty acids) substrate resulted in a bio-wax which contained 96% of C_{27}–C_{35} ketones at 99% conversion, showing very high ketone selectivity, supporting the side product analysis of unsaturated fatty acid di/trimerization side reactions for ketonization of the non-hydrogenated PFAD (Fig. S13 and S16†).

In summary, hydrogenation of unsaturated fatty acid substrates prior to ketonization may be recommended if very high ketone selectivity (>90%) is important for the target application. As will be shown in section 3.4, this is not the case for the particular application of this study.

The relative composition of the head space gasses (besides N_2 as flushing agent) was analysed offline *via* GC after a batch reaction with full PFAD conversion, showing that nearly all of the head space gas consisted of CO_2 (96 vol%), in expectation with the ketonization reaction equation (eqn (1)). Additionally, trace amounts of light hydrocarbons (1.9 vol%) and CO (2.1 vol%) were also detected, which can be formed from minor side-reactions such as cracking, deoxygenation or (reverse) water–gas-shift reactions. No hydrogen gas was detected and the liquid (water) phase was not collected for analysis after reaction. To complete the total mass balance, the absolute amount of CO_2 and water were calculated based on the reaction stoichiometry and the amount of ketone formed (and thus the actual measured ketone selectivity).

Finally, some physical properties of the solid PFAD wax product were measured to complete the energy balance of the ketonization process. The melting point and heat capacity values of the PFAD based bio-wax were determined using differential scanning calorimetry (Fig. S17†). The melting point peak is situated around 71 °C, while the overall melting profile is broad between approximately 55 and 75 °C. This is a direct result of the different carbon chain lengths and presence of various (un)saturated isomers in the C_{27}–C_{35} ketone mixture. Finally, the average heat capacity of the liquid wax

Table 4 Full mass balance for complete ketonization conversion of 40 g PFAD

Input	Quantity (g)	Output	Quantity (g)
Myristic acid	0.5	C_{27} ketone	0.1
Palmitic acid	19.3	C_{29} ketone	0.5
Stearic acid	1.7	C_{31} ketone	10.4
Oleic acid	15.3	C_{33} ketone	12.8
Linoleic acid	3.2	C_{35} ketone	3.5
		C_{36} dimers and C_{54} trimers	8.7
		C_{15}–C_{17} hydrocarbons	0.36
		CH_4	0.01
		C_2H_4	0.01
		C_2H_6	0.01
		C_3H_8	0.01
		C_{4+}	0.01
		CO	0.03
		CO_2	2.5
		H_2O	1
Total substrate	**40**	**Total products**	**39.94**

product was measured at 3.28 J g^{-1} K^{-1} between 80–100 °C (above melting point, see ESI†).

3.4. Hydrophobization application of ketone bio-waxes

We also created ketone bio-waxes from other commercial fatty acids, of which we have previously reported the hydrophobization performance.[44] These include animal fat (59% FFA, by-product of chemical animal fat refining), coconut and palm kernel fatty acids (compositions in Table S1†). Their fatty acid profiles are significantly different, which evidently is reflected in the composition of the resulting ketone mixtures. After full conversion, the coconut and palm kernel derived bio-waxes consisted of 97 and 96% ketones, respectively, mainly comprised of shorter saturated C_{23}–C_{27} ketones. As a result, the 53 °C melting point of the palm kernel bio-wax is considerably lower than that of the PFAD bio-wax (Fig. S18†). This shows that depending on the desired physicochemical properties of the end product, ketonization allows targeted selection of the appropriate biomass feedstock.

The ketone bio-wax originating from PFAD was tested as a hydrophobization agent for wood composite materials in an aqueous wax emulsion. This is an important industrial treatment to reduce the penetration of water into various (construction) products, by minimizing swelling and increasing the resistance to moisture and water uptake. While typically petroleum derived paraffin waxes are used for this application, here we investigated and compared the performance of the bio-based ketone wax. This also means that no additional hydrodeoxygenation step was performed to convert the ketones into their corresponding alkane analogues.

To determine the hydrophobization performance of PFAD bio-wax, wooden panels were first treated with its aqueous wax emulsion and subsequently submerged in a water column for 2–24 hours. Afterwards, both the water uptake and degree of swelling were determined and compared to the other bio-waxes and three commercially available fossil based benchmarks (Table 5). Wax 1 is a solvent dewaxing product of a SN150 base oil, which is known for its excellent water repellent properties. Wax 2 originates from the solvent dewaxing of SN300 or SN350 base oil streams and has an intermediate performance regarding water repellence of particle and chipboards. Finally, wax 3 is a slack wax known for its overall lower quality in this kind of application. First of all, the results of Table 5 show an increased resistance to water for the PFAD bio-wax coated panels as the water uptake and swelling thickness values are lower than those of the blank control sample. When the application results of the PFAD bio-wax are compared to those of waxes 1–3, better or at least similar water repellence properties are obtained compared to wax 1, which is known in the industry for its excellent performance. This was also the case for the other bio-based waxes, of which the animal based product performed slightly better than the others.

Besides its hydrophobization performance, the thermal stability of the PFAD bio-wax was determined under oxidative conditions (O_2) up to 750 °C *via* TGA (Fig. S19†). The primary weight loss starts to occur at the onset temperature of 200 °C, while the remaining 25 wt% degrades between 300–500 °C, similarly to the TGA profile of the commercial dimer acid mixture. The thermal stability profile of the bio-wax is satisfactory and comparable to those of a standard C_{32} alkane and the commercial fully refined paraffin wax used in this kind of application. Based on our findings, aqueous phase emulsions containing biomass derived ketones have the potential to replace the current fossil based standards.

3.5. Process design

A realistic process design with mass and energy balances is the basis of any dedicated LCA. Based on the lab scale results, we developed an integrated industrial process scheme using both a scaling-up framework from literature[67] and expertise from industry specialists. With an initial annual bio-wax production capacity of 5 kiloton, this design starts with feedstock unloading from a transport truck, by heating from around 15 to 70 °C to enable liquid feedstock pumping to a storage vessel that is kept at constant 70 °C (Fig. 2). These practices are suggested by the oleochemical industry for practical fatty acid handling.[68] The feedstock is then pre-heated and pumped to the reactor, TiO_2 catalyst is added, while continuous venting with N_2 gas creates an inert reaction atmosphere and removes CO_2, H_2O and other gaseous by-products. The desired ketonization temperature can be reached by a thermal oil system, using

Table 5 Application test of bio-wax ketones in aqueous wax emulsions for hydrophobization of wooden panels

	Blank[a]	PFAD[d]	Animal[e]	Coconut[e]	Palm kernel[e]	Wax 1[e]	Wax 2[e]	Wax 3[e]
Wt% ketone in solid bio-wax	NA	75	61	97	96	NA	NA	NA
Water repellent properties								
Water uptake[b] 2 h	81	27	19	26	27	19	26	59
Water uptake 5 h	83	36	28	39	40	33	38	73
Water uptake 24 h	90	59	52	63	64	71	69	86
Thickness swelling[c] 2 h	16	8	6	7	7	6	7	13
Thickness swelling 5 h	17	11	8	10	10	8	9	16
Thickness swelling 24 h	18	17	17	17	18	17	19	19

[a] Without any aqueous emulsion treatment. [b] Measured as percentage increase in weight of the wooden panel test sample after submersion in water. [c] Measured as percentage increase in thickness of middle part of wooden panel after submersion in water. NA: not applicable. [d] This work. [e] Ref. 44.

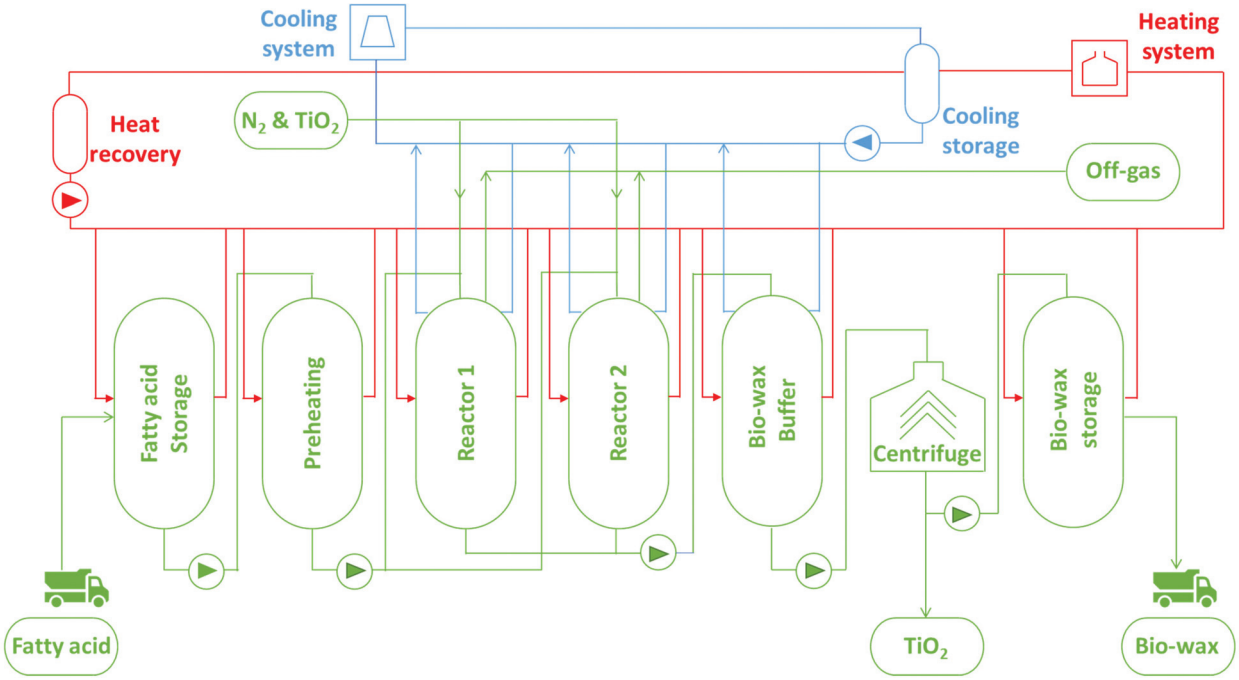

Fig. 2 Proposed industrial ketonization process scheme with detailed indication of mass and energy flows.

natural gas for the required thermal energy. A second identical reactor was included in this design to efficiently transfer the thermal energy of the first reactor during cooling down when the catalytic ketonization reaction is completed. The second reactor can then utilize this thermal energy *via* an integrated heat recirculation loop, which can be achieved *via* cooling technology which includes adiabatic cooling towers with water/steam circulation.

Constant N_2 venting at low to moderate pressures (5–10 bar) ensures fast and full PFAD conversion in the liquid phase due to continuous CO_2 and H_2O removal. Nitrogen is purged through the liquid phase using established technologies such as integrated systems in the mechanical stirrer. The vapour pressure of pure palmitic acid, which is the main component of PFAD, was calculated *via* the Clausius–Clapeyron equation and has a value of around 10 kPa at 350 °C and 10 bar N_2 pressure (ESI†).[69] As a result, potential feedstock loss *via* the vapour phase is already limited significantly by the operating conditions. Furthermore, during catalytic operation the vapour phase is continuously removed and passed through a condenser at the outlet, which is a system similar to that of the lab scale operation. Hereby, unreacted fatty acids (if any are present in the outlet stream) are immediately sent back to the reactor by condensation.

Several treatment options exist for the remaining outlet mixture of N_2, CO_2, H_2O, CO and hydrocarbons. They can be emitted as such, separated for recycling of process N_2 or sent to an incinerator system for full conversion to a mixture of N_2, H_2O and CO_2 using additional air in a regenerative thermal oxidation (RTO) unit for potential thermal energy recuperation and possible emission reduction. Regarding the latter, in section 3.6.2 it will be shown that there is no global warming potential reduction *via* off-gas incineration. This is due to the very low total amount of CO and trace hydrocarbons in the gas outlet. Based on the outlet composition and associated reported lower heating values,[70] complete combustion of the hydrocarbons and CO would generate 5.4% of the total energy requirement per batch. This is an upper value and does not take into account the thermal and electrical energy necessary to operate such an incinerator system (typically operating around 850 °C). Also, additional mass input would be required, as well as additional capital and operating costs. Based on the balance between these three considerations (no emission reduction, limited energy recuperation, additional costs), the off-gas incineration was omitted in the base case process design.

To separate the TiO_2 catalyst from the wax product, the reactor effluent is sent to a heated (disk stack) centrifuge system operating at 100 °C. An intermediate product stock is installed to first increase the total amount of product before applying this separation step. After separation, the catalyst is recuperated for reuse. Based on the lab scale results and industry expertise, the amount of catalyst loss for this step was set at 3%. A wax product loss of 1% was accounted for in this design.

A more detailed overview of the inventory data and accompanying assumptions to compose the overall mass and energy balances is summarized in Table S2.† An important note must be made here on the reaction enthalpy. While the endothermic standard enthalpy of reaction is 30 kJ mol^{-1} for palmitic acid ketonization,[34] tabulated thermodynamic values are not available for the ketonization reaction at 350 °C. Based on the

Table 6 Energy balance for conversion of one PFAD batch (3656 kg) in the designed ketonization process scheme

Process step	Energy requirement (kJ per batch)	Description
PFAD unloading and storage	Thermal: 718 845	Heating from 15 to 70 °C
	Electricity: 3373	Includes pumping
Ketonization	Thermal: 4 350 490	Includes heating to 350 °C and endothermic reaction enthalpy
	Electricity: 86 400	Includes pumping, mechanical stirring and nitrogen venting[67]
Heat transfer	Thermal: −2 310 390	Recuperated thermal energy after reaction (cooling to 100 °C)
	Electricity: 334 800	Includes cooling and heating circulation
Product storage and centrifugation	Thermal: 48 916	Includes temperature losses of 2 °C during centrifugation and pumping
	Electricity: 111 600	Includes pumping and centrifugation step[67]
Total balance	Thermal: 2 807 861	With heat transfer integration
	Electricity: 536 173	

temperature dependence of the heat capacities of substrates and products,[71,72] we have estimated this parameter to be around 55 kJ mol^{-1} at 350 °C (see ESI†).

The energy balance of the process is summarized in Table 6, where for each step a distinction is made between thermal energy (heating and cooling) and electrical energy (pumping, compression, centrifugation, *etc.*). The ketonization of one batch PFAD requires 2 807 861 kJ of net thermal energy (780 kW h). The total required electrical energy is significantly lower at 536 173 kJ (149 kW h). The ketonization reaction is the most energy intensive step due to the reaction temperature of 350 °C and its endothermic character. For this energy balance, the highest value of 55 kJ mol^{-1} was used to avoid any underestimation (Fig. S20†). For reaction enthalpy values at 350 °C of 30 and 55 kJ mol^{-1}, the total energy requirement for ketonization of one PFAD batch is 827 and 929 kW h, respectively. This indicates that the availability of thermodynamic values at elevated temperatures would be highly valuable for the ketonization reaction. Regarding energy integration and recuperation, Table 6 shows that the heat transfer system recuperates 45% of the total thermal energy cost, significantly lowering the net energy requirement.

Although no economic study is aimed in this work, we have estimated the manufacturing cost of 1 ton bio-wax by taking into account the input costs of PFAD, TiO_2, N_2 and energy (Table S3†), as well as the catalyst separation, recovery and associated losses.[73–77] A varying TiO_2 price between €1000–15 000 per ton results in a bio-wax production cost of €724–1136 per ton (Fig. S21†) at constant prices for the other inputs. The use of a selective, active and reusable heterogeneous catalyst is thus important for the process economics as these "back on the envelope" calculations reveal that the total ketone bio-wax price is heavily influenced by the TiO_2 catalyst.

3.6. Environmental sustainability monitoring

The environmental impact of bio-wax production *via* ketonization of fatty acids is studied twofold. First, the Green Chemistry principles, the basis of all sustainability measures of a chemical reaction, are evaluated to provide insights into the atom efficiency and waste generation. If desirable scores such as high atom economy and carbon efficiency are achieved, this is followed by a detailed cradle-to-grave life cycle assessment, as this reflects a much broader impact of the proposed technology on the environmental sustainability. Certainly, promising Green Chemistry results do not necessarily guarantee products with low environmental impacts. Conversely, renewable chemicals with low environmental impacts should be obtained from chemical reactions with satisfactory Green Chemistry scores.

3.6.1. Green Chemistry. The principles of Green Chemistry can be summarized in the following working definition proposed by Roger A. Sheldon: "Green Chemistry efficiently utilises (preferably renewable) raw materials, eliminates waste and avoids the use of toxic and/or hazardous reagents and solvents in the manufacture and application of chemical products".[78] Afterwards, Anastas and Zimmerman reformulated these principles from an engineering perspective. This includes minimizing the consumption of fossil energy, waste production and use of toxic auxiliaries, and incorporating renewable energy generation.[79] The use of catalysis to improve selectivity and conversion rate is also highlighted. In this study, the presence of the TiO_2 catalyst is essential for the formation of wax ketones as we have observed no thermal ketonization of fatty acids.

Seven Green Chemistry measures were calculated for the ketonization of PFAD (Table 7). The *E*-factor has a value of 0.15, meaning that 0.15 kg of "waste" (H_2O, CO_2 and trace gasses) is produced per kg bio-wax. This value is very low compared to typical *E*-factors of bulk chemicals (<1–5), fine chemicals (5–50) and pharmaceuticals (25–100), while oil refining

Table 7 Overview of Green Chemistry results for the ketonization of PFAD

Green Chemistry parameter	PFAD ketonization	Ideal value	Comments
E-factor	0.15	0	0.15 kg waste per kg ketone wax
Atom economy %	89	100	High
Effective mass yield %	87	100	High
Mass intensity	1.15	1	Good
Mass productivity %	87	100	High
Carbon efficiency %	95	100	Very high
Reaction mass efficiency %	87	100	High

processes can achieve values lower than 0.1.[78] The mass intensity (MI) of the ketonization has a value of 1.15 (*E*-factor plus 1). Taking into consideration the ideal *E*-factor and MI values of 0 and 1, respectively, it can be stated that the ketonization is not wasteful nor mass intensive. This is in line with the reaction equation, forming one molecule of CO_2 and H_2O per two fatty acid substrate molecules (regardless whether long or short-chain reagents are used). This also implies that an increase in substrate chain length will result in better scores for atom economy and carbon efficiency measures. For PFAD (predominantly C_{16}–C_{18}) this leads to a high theoretical atom economy of 89% and an even greater carbon efficiency of 97%. In contrast to this study, most ketonization research has focussed on C–C coupling of short-chain carboxylic acids to upgrade pyrolysis bio-oil towards fuels. For example, the theoretical atom economy and carbon efficiency values for the ketonization of acetic acid to acetone are 48 and 75%, respectively, which are considerably lower than the scores of fatty acid valorisation. This shows that critical selection of a suitable carboxylic acid feedstock is crucial. The effective mass yield of bio-wax production reaches 87% and equals both the mass productivity and the reaction mass efficiency since no solvent is used in the liquid phase process. Minimizing or better yet avoiding solvent use is indeed an effective strategy to lower the environmental burden of a chemical reaction and process scheme.

Overall, these results indicate that ketonization of long-chain fatty acids is a chemical reaction with desirable Green Chemistry measures. Because of these high atom economy and carbon efficiency values, the necessary condition is met to perform a detailed cradle-to-grave life cycle assessment. Here, the broader environmental impact of the ketonization technology and final bio-wax product will be determined.

3.6.2. Life cycle assessment. Based on life cycle assessments of other bio-based chemicals, such as linear alkylbenzenesulphonate and fatty alcohol sulphate surfactants from vegetable oils,[80] and behenyl behenate ester from rapeseed oil,[81] the importance of expanding the system boundaries to a cradle-to-grave approach is clear. This tends to be the most reliable, comparable and representative system boundary.[39,82] In our comparative study, the cradle-to-grave system boundaries include extraction or harvesting of input resources, processing to produce wax, end-of-life and the transport requirements between the different stages. This ensures that all emissions are included and burden shifting across stages is avoided. The begin-of-life phase for PFAD bio-wax coincides with the cultivation of palm trees, while the extraction of fossil oil is regarded as the begin-of-life stage for paraffin wax. The end-of-life scenario is assumed to be incineration for both, because the wax-coated products (*i.e.* wood panels, textiles *etc*.) will ultimately be incinerated in all probability. This latter assumption is also supported by recommendation of industry experts.

As the gate-to-gate data (of the ketonization process) are not yet optimized to the same degree as the paraffin benchmark process, the up-scaled mass and energy balances in this study may lead to greater environmental impacts for bio-wax than in the case of optimized industrial implementation. Nevertheless, this LCA aims to offer an insightful comparison between fossil paraffin and bio-wax and to highlight the most important areas that are determining the overall environmental sustainability of such bio-wax products.

Flow diagrams and system boundaries. Fig. 3 shows the flow diagram and cradle-to-grave system boundaries (orange dotted line) of the fossil-based paraffin wax life cycle as studied in this work. The production of conventional paraffins involves numerous energy and solvent intensive steps in which crude oil needs to be refined towards a clean, pure (white) paraffin wax. In short, a small part of the vacuum distillate of the refinery (from the middle trays) is sent to the base oil processing unit where dewaxing of lube oil yields slack waxes.[50] Today, the most common technique is solvent dewaxing in which organic solvents are used as diluents in 2–4 times excess. These typically include methyl ethyl ketone (MEK), toluene, dichloroethane, benzene, propane and acetone, some of them which have potential adverse effects concerning human and ecological toxicity and persistency. The vacuum distillate fraction is washed with an excess amount of solvents and subsequently cooled leading to the crystallization of slack wax, which is a dark mixture of oil and wax. Due to the severe dilution and cooling requirements, this step involves the highest cost in the lube oil processing.[83] To further de-oil this slack wax, a solvent refining washing process with organic solvents is performed to create two product fractions: the solvent containing the oil, and the wax product with a small amount of remaining solvent. This solvent is then removed from the wax and recycled. In order to obtain the desired low oil content, the de-oiling process may be repeated 2–3 times. To eliminate unwanted odours and colours, the de-oiled wax is further purified with activated clay in either a filter press or a rotary drum. Removal of the last remaining impurities to obtain refined paraffin wax requires additional energy-intensive adsorption (using bleaching earth, activated carbon, silica gel and bauxites) or chemical treatments such as hydrogenations, oxidations, condensations, polymerizations, sulfonations *etc*.[83,84] Finally, the paraffin wax can be used in an aqueous wax emulsion for hydrophobization of (wooden composite) materials. Accordingly, the functional unit (FU) has been defined as 1 kg of petroleum wax ready to use in a wax emulsion product.

Fig. 4 illustrates the flow diagram and cradle-to-grave system of the PFAD bio-wax. It includes the cultivation (cradle) of the palm oil bearing fresh fruit bunches (FFB) and all the subsequent processing steps required to reach the gate of the system, being refined palm oil PFAD (Experimental section ESI† for more detailed description).[85] After transportation of PFAD to the designated ketonization plant, the main steps of the process occur as outlined in sections 3.2–3.5. Besides PFAD, the production of the N_2 and TiO_2 inputs have also been included (detailed description in ESI†). Similarly to the paraffin wax, the functional unit (FU) has been defined as 1 kg of bio-wax ready to use in a wax emulsion product.

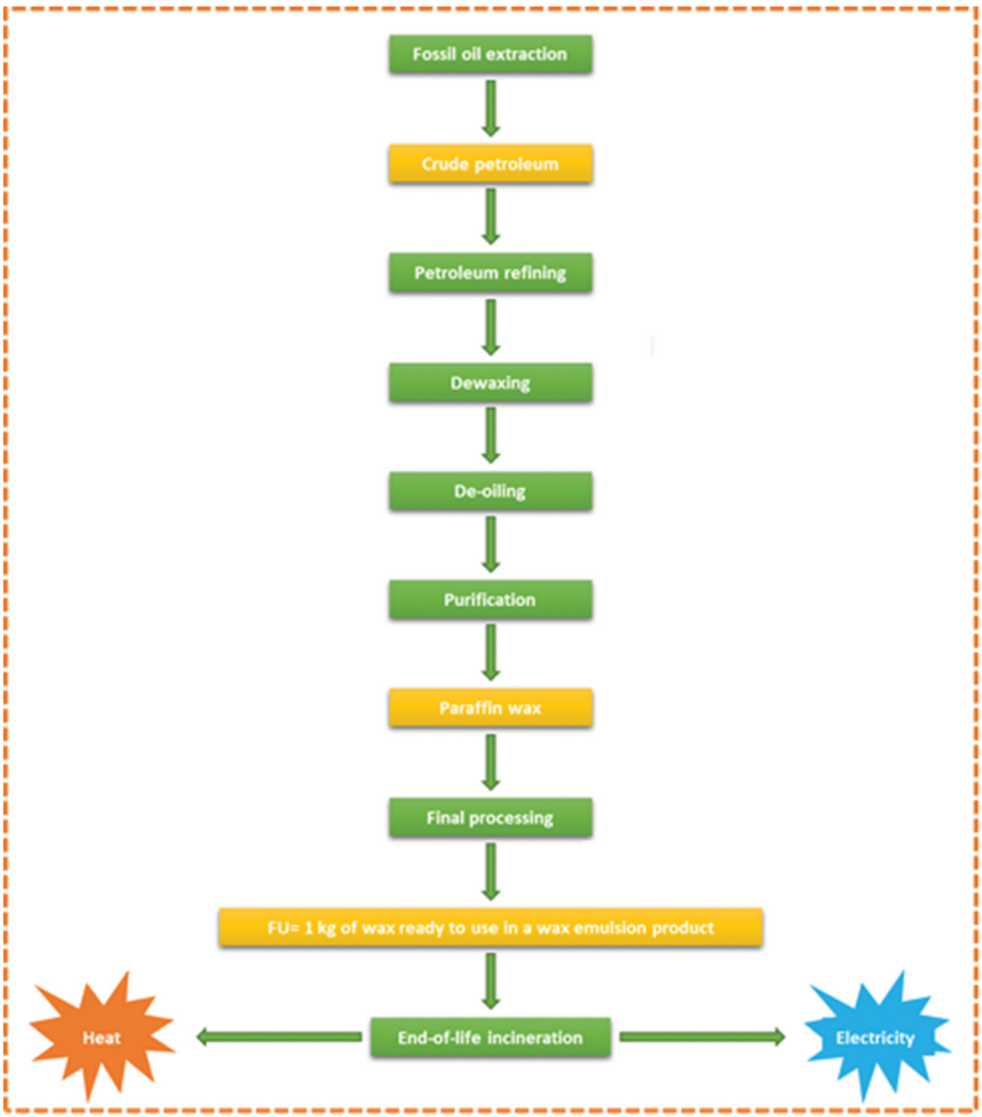

Fig. 3 Flow diagram with system boundary (orange dotted line) of the paraffin wax life cycle starting from fossil oil extraction until the end-of life incineration.

Base case LCA. The mass inventory of the base case scenario for PFAD bio-wax is summarized in Table S4.† Here, the partial retention of activity of the TiO_2 catalyst has been taken into account, as well as product and catalyst losses during process operation. As a result, the production of 1 functional unit (1 kg bio-wax) requires 1.11 kg of PFAD feedstock. To calculate the impact of the latter, the production of refined palm oil was used as starting point. Palm fatty acid distillate is a 4.5 wt% by-product of the crude palm oil refining process, implicating that 1.11 kg PFAD requires the production of 24.7 kg of RPO. In this study, market prices of €600 and €770 were used per ton of PFAD and refined palm oil (RPO), respectively.[75,76] This leads to an economic allocation factor of 3.41% for PFAD, and the impact modelling factor for 1 FU equals 84.1% of RPO (Table S5†).

The overall base case LCA results are shown in Table 8, where all impact scores are expressed in terms of 1 functional unit. For fossil paraffin wax, the climate change impact (CCI) equals 2.83 kg CO_2 eq. per FU, which can be broken down into more detail to investigate the importance and contribution of the different stages in the life cycle (Fig. S22†). The paraffin production (1.09 kg CO_2 eq. per FU) and end-of-life (EoL) incineration (3.13 kg CO_2 eq. per FU) would imply an overall value of 4.22 kg CO_2 eq. per FU, which is 49% higher than the tabulated value. However, it is important to include energy recuperation as significant amounts of electricity (−0.69 kg CO_2 eq. per FU) and thermal energy (−0.71 kg CO_2 eq. per FU) can be recovered during the EoL incineration, reducing the net carbon footprint of the overall fossil paraffin wax life cycle.

For the CCI of bio-wax, a distinction was made between models which exclude and include biogenic carbon as a contri-

Fig. 4 Flow diagram with system boundary (orange dotted line) of the bio-wax life cycle starting from PFAD as a by-product of palm oil cultivation until the end-of life incineration.

butor to climate change, respectively. In the first model, which is the most common methodology in LCA on bio-based products, the amount of CO_2 captured during crop cultivation *via* photosynthesis is assumed to be equal to the CO_2 emission during the end-of-life phase (carbon neutrality assumption). As a result, they are excluded from the analysis and the CCI of PFAD bio-wax is 2.57 kg CO_2 eq. per FU, 9.2% lower than the CCI of paraffin wax. In contrast, its CCI is 3.9% higher when

Table 8 Overview of the base case LCA results for 1 FU of fossil paraffin wax (LCA_p) and bio-wax (LCA_b)

Impact category	Fossil paraffin wax	Bio-wax
Climate change, excl. biogenic carbon [kg CO_2 eq.]	2.83	2.57
Climate change, incl. biogenic carbon [kg CO_2 eq.]	2.83	2.94
Freshwater consumption [m^3]	0.0014	0.067
Freshwater eutrophication [kg P eq.]	1.04×10^{-6}	5.72×10^{-5}
Human toxicity [kg 1,4-DB eq.]	0.24	0.88
Photochemical ozone formation, ecosystems [kg NO_x eq.]	5.75	6.19
Photochemical ozone formation, Human Health [kg NO_x eq.]	3.57	3.84
Terrestrial acidification [kg SO_2 eq.]	1.13×10^{-3}	7.93×10^{-3}
Terrestrial ecotoxicity [kg 1,4-DB eq.]	0.26	2.19

biogenic carbon is included as a contributor to climate change (2.94 kg CO_2 eq. per FU). The carbon neutrality assumption is a hot topic in the field of LCA, sparking many debates on its validity.[38,39] It can significantly alter the LCA results, often (wrongfully) reducing the impact of the bio-based products. Excluding biogenic carbon as a contributor to climate change may be valid in some cases, however. Specifically for palm cultivation, it has been shown that CO_2 uptake and emissions fluctuate as a function of the plantation age.[86] While young plantations act as net carbon emitters due to their lower photosynthesis rates and higher soil emissions (often more recent deforestation), mature plantations may reach a more carbon neutral situation. Furthermore, the carbon neutrality assumption is also heavily dependent on the geographical location of cultivation (Malaysia in our case) and the associated land use change emissions originating from the conversion of (primary/secondary) forest, grasslands, *etc*. into agricultural land.[87] For the specific case of Malaysia, this often concerns land areas which were originally covered with primary forest. Indeed, deforestation of these areas were and still are contributing to land use change emissions. Lastly, the carbon neutrality assumption may be specifically valid for short-lived materials, while it may actually overestimate the CCI of a product when the biogenic carbon remains captured in a long-lived stable product. To avoid purposefully underestimating the CCI of a bio-based product, we initially conclude that it is not advisable to assume carbon neutrality.

A more detailed breakdown of the cradle-to-grave CCI of PFAD bio-wax is presented in Fig. 5. The production of PFAD (0.91 kg CO_2 eq. per FU) and the end-of-life incineration (3.13 kg CO_2 eq. per FU) are the main contributors to climate change. Regarding the in- and exclusion of biogenic carbon, it is clear that the ΔEoL (3.13 kg CO_2 eq. per FU) and ΔPFAD production (2.82 kg CO_2 eq. per FU) values are not equal (ΔCCI of 0.31 kg CO_2 eq. per FU). The most important underlying reason is the emission of biogenic gasses other than CO_2, which have a higher relative contribution to climate change. In fact, 0.017 kg of biogenic methane is emitted during production of 1 kg PFAD. This methane is typically released during anaerobic open pond treatment of the palm oil mill effluent (POME). As 1 kg of biogenic methane is equivalent to approximately 25 kg of CO_2 (over 100 years), these methane emissions contribute around 0.47 kg CO_2 eq. per FU. This value is in good agreement with the ΔCCI of 0.31 kg CO_2 eq. per FU, which also implies that when these biogenic methane emissions can be avoided (see further), the impact on climate change of PFAD bio-wax can be reduced significantly.

These breakdown results also show that the CCI values linked to the total energy required for the ketonization reaction (0.15 kg CO_2 eq. per FU) and the production of the TiO_2 catalyst (0.07 kg CO_2 eq. per FU) are rather small, contributing 5% and 2.1% to the total impact, respectively. Due to the pioneering nature of this work, direct comparison of these carbon footprints with comparable literature on ketonization is not possible. However, the impact on climate change of the ketone bio-wax is in the same order of magnitude as those of other reported types of bio-based waxes. In one study, the environmental impact of behenyl behenate ($C_{44}H_{88}O_2$) ester originating from rapeseed oil was determined.[81] The economic allocation and cradle-to-grave approach resulted in CCI values of 1.9 and 3.7 kg CO_2 eq. per FU for the ester and paraffin wax, respectively (with neutrality assumption). A second study investigated the cradle-to-grave carbon footprint for linear alkylbenzenesulfonate (LAS, a surfactant) using petroleum, coconut oil (CO) and palm kernel oil (PKO) derived paraffin.[80] The cradle-to-grave emissions reported for PKO and CO gave very similar results for the bio-based LAS, *viz*. 1.93 and 1.89 kg CO_2 eq. per kg LAS, respectively (mass allocation). These were 46.2% and 47.3% lower than petroleum-based LAS (3.58 kg CO_2 eq. per kg LAS). However, these numbers omitted contributions from land use change (LUC) and were calculated under the assumption of biogenic carbon neutrality at the end-of-life. Incorporation of LUC, for instance by the conversion of primary and secondary forests, would lead to a significant increase in emissions, resulting in 2.8 kg CO_2 eq. per kg LAS.

For the terrestrial acidification impact category, the production of PFAD bio-wax is accompanied by 7.93×10^{-3} kg SO_2

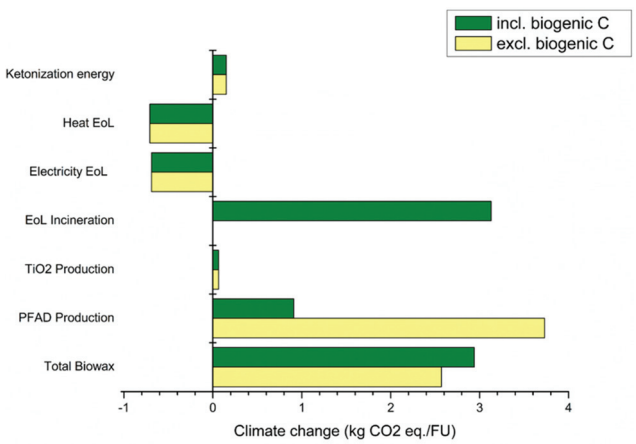

Fig. 5 Detailed breakdown of the CCI of PFAD bio-wax.

Table 9 Overview of hotspot analysis with associated contributions to the LCA impact categories per FU

Impact category	Hotspots (% contribution per FU)		
	PFAD	TiO_2	Incineration
Climate change, incl. biogenic carbon [kg CO_2 eq.]	31	2.2	59
Freshwater consumption [m^3]	95	3.7	0.67
Freshwater eutrophication [kg P eq.]	58	43	−3.3
Human toxicity [kg 1,4-DB eq.]	84	16	−0.21
Photochemical ozone formation, ecosystems [kg NO_x eq.]	13	0.02	86
Photochemical ozone formation, human health [kg NO_x eq.]	13	0.02	87
Terrestrial acidification [kg SO_2 eq.]	102	16	−19
Terrestrial ecotoxicity [kg 1,4-DB eq.]	99	10	−9.4

eq. per FU, while the production of paraffin wax emits 1.13×10^{-3} kg SO_2 eq. per FU. When these values are broken down for bio-wax, the production of both PFAD and TiO_2 are identified as the main contributors to this impact category. For PFAD, this is due to the agricultural emissions during palm cultivation (use of fertilizers), while for TiO_2 the mining of ilmenite ore and the use and disposal of high quantities of sulphuric acid during the production process are the main reasons (ESI†).[88] The eutrophication of freshwater bodies (FE) is a well-known environmental problem that induces a cascade of ecological impacts. The FE impact of bio-wax equals 5.72×10^{-5} kg P eq. per FU, while the FE value of paraffin wax is lower at 1.04×10^{-6} kg P eq. per FU. For bio-wax this mainly originates from the production of the feedstock and catalyst. The high impact on eutrophication of palm cultivation is in line with expectations as it concerns an agricultural process associated with the emission of nutrients through the use of fertilizers. Electricity generation from brown coal mining, ilmenite mining and thermal energy consumption are the driving factors to explain the high FE contribution of the TiO_2 catalyst. Photochemical ozone formation (POF) arises from the UV light-induced reaction of nitrogen oxides (NO_x) with non-methane volatile organic carbons (NMVOC). Incineration and combustion processes for waste treatment and energy generation are often the main contributors to POF as these processes can generate both NMVOC and NO_x. As shown in Table 8, the difference between bio-wax (10.03 kg NOx eq. per FU) and paraffin wax (9.32 kg NOx eq. per FU) is rather small. While paraffin and PFAD production are responsible for 0.6 and 1.1 kg NO_x eq. per FU, respectively, the EoL incineration is the life cycle step with the highest POF impact by far as it is almost solely responsible for the remaining fraction of the total POF impact category.

Hotspot and sensitivity analyses. The processes within the LCA that contribute the most to the overall environmental impact of the life cycle are defined as hotspots or weak points. To identify these, a hotspot analysis was conducted with a threshold of 10% (steps contributing more than 10% to a certain impact category of the total life cycle). This analysis resulted in the identification of three hotspots: PFAD production, TiO_2 production and end-of-life incineration (Table 9). These life cycle steps are to be prioritized when aiming to reduce the overall environmental impact of the cradle-to-grave life cycle. Additionally, a sensitivity analysis was performed on the most important input parameters related to these hotspots to gain further insight into their contributions. The production of PFAD feedstock has a high impact for multiple categories, including climate change, freshwater eutrophication, human toxicity, photochemical ozone formation, terrestrial acidification and terrestrial ecotoxicity. The sensitivity analysis shown in Fig. 6 depicts the difference in the overall impact results when 110% of the base case scenario substrate amount is required for the production of 1 FU. Practically, this corresponds to the situation where the bio-wax yield of the ketonization process is reduced by 10% due to incomplete substrate conversion, product losses, *etc*. Clearly, the necessary amount of fatty acid substrate is a sensitive parameter that

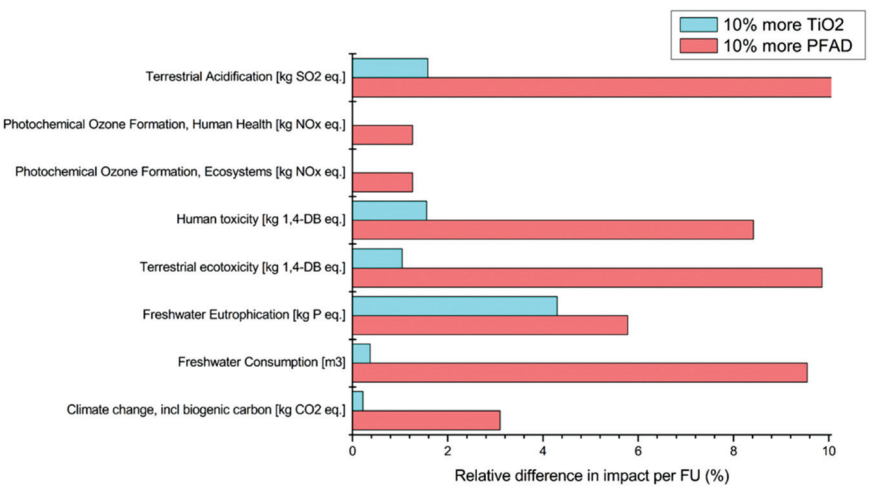

Fig. 6 Sensitivity analysis on the use of PFAD and TiO_2 for the production of 1 functional unit.

heavily influences the total impact of the functional unit. This emphasizes again that substrate choice is paramount, combined with the development of an efficient and selective ketonization process. We have already shown the latter in sections 3.2–3.5 of this work, as full substrate conversion can be reached with the expected stoichiometric amounts of H_2O and CO_2 as by-products next to the solid bio-wax (with a ketone composition depending on starting substrate). As such, a scenario which only requires 90% of the base case substrate amount per FU is not possible in this case.

As a robust conclusion from this hotspot analysis of PFAD production, it can be stated that palm cultivation and refining are accompanied with large emissions to soil, air and water. Therefore, these processes have high scores for multiple impact categories. The cultivation and LUC emissions of different forms of carbon (CO_2, CH_4, NMVOC), phosphorus (P and PO_4^{3-}), nitrogen (NO^{2-}, NO^{3-}, NH_3, NO_x, N_2O...) and pesticides play an important role in determining the impact of the final bio-wax product. To reduce the overall environmental impact of ketone bio-waxes for these impact categories, the development of more sustainable agricultural processes is required in the future. For example, more efficient use of water, fertilizers, herbicides, pesticides and increased utilization of renewable energy sources are advised.

The production of the TiO_2 catalyst is the second hotspot in the overall life cycle of ketone bio-wax, with high contributions to freshwater eutrophication, human toxicity, terrestrial acidification and ecotoxicity (Table 9). The sulphate process requires 20.4 MJ kg^{-1} TiO_2 of thermal energy and 4.66 MJ kg^{-1} TiO_2 of electricity. A part of this energy is generated *via* brown coal mining and other polluting pathways, which implies impacts on climate change, freshwater eutrophication, terrestrial acidification and toxicity. Furthermore, attention needs to be given to the use and disposal of large quantities of sulphuric acid. Indeed, 1 kg TiO_2 requires 2.38 kg of sulphuric acid and generates around 3.85 kg of gypsum waste.[88] The environmental footprint of titanium dioxide therefore strongly depends on the geographical location, type of manufacturer, mining conditions, extraction technologies, energy efficiencies, *etc*. to convert the raw materials into functional catalysts. To further investigate its influence on the environmental impact of bio-wax, a sensitivity analysis was carried out which examines the difference in overall impacts when 10% more TiO_2 is required for the production of 1 functional unit (Fig. 6). Practically, this may imply a scenario where the catalytic activity of TiO_2 is reduced. The presented results suggest that the catalyst loading is a sensitive parameter, considering that an average value of 0.029 kg TiO_2 is required to produce 1 kg bio-wax (Table S4†). Oppositely, this also implicates that a decrease of 10% in catalyst loading can lead to a reduction of the overall impacts of the bio-wax product. Regarding catalyst production, manufacturers should aim on reducing the total energy requirement, as well as incorporating the use of more renewable energy sources. Furthermore, more efficient use and recycling of reagents such as sulphuric acid, in combination with reduction of waste generation, can contribute to lower environmental impacts for TiO_2. For the ketonization process in particular, careful economical management (use and reuse) and further optimization of performance (activity and stability) of the titanium dioxide catalyst is recommended to decrease the overall environmental impact of the bio-wax product. Additionally, improved activity and stability of the active material can also greatly benefit the overall economics of the ketonization process by reducing the catalyst cost, as discussed in section 3.5.

The end-of-life incineration is the third hotspot of the bio-wax life cycle due to its very high contribution to climate change and photochemical ozone formation (Table 9). In contrast, the thermal energy and electricity that are recovered during this step lower the net cradle-to-grave impacts for freshwater eutrophication terrestrial acidification and terrestrial ecotoxicity. These results show that the production of durable and stable long living materials is crucial, together with selection of the most suitable end-of-life phase. In this regard, efficient recycling of both mass and energy contents is vital at this end stage (circular economy), since it can heavily influence the true cradle-to-grave impacts of a product.

As shown in this work, the hotspots of LCA_b of PFAD are mainly located outside the gate-to-gate boundaries (ketonization process). This also emphasizes the importance of choosing representative system boundaries in line with the goal and scope of the LCA study. When one wants to solely evaluate the environmental impact of a technological process, a gate-to-gate scenario can be used. However, when the aim is to assess the overall environmental impact of bio-based product such as wax, a cradle-to-grave approach is required.

Scenario analyses. So far we have selected very strict conditions for the base case LCA scenario to avoid any underestimation of the environmental impact of the PFAD bio-wax. As discussed at the start of this section, the specific cultivation system of palm could have a significant influence on the LCA outcome. Therefore, we have analysed different scenarios to gain a broader understanding on this subject in order to formulate informed advices (Fig. 7).

First, a scenario was included where PFAD does not lead to LUC emissions. At 0.38 kg CO_2 eq. per FU, this scenario equals a 87% reduction of the base case scenario and results in a 7.4 times lower CCI than paraffin wax. For this specific case, the contribution of PFAD production is −1.7 kg CO_2 eq. per FU (including biogenic carbon), which means that the biomass cultivation step acts as a net carbon sink. The importance of taking the correct LUC emissions into account, if necessary, is emphasized by this scenario. In this context, a study by Flynn *et al.* calculated LUC emissions of the top 20 palm oil producing countries (Table S6†).[89] Here, the value of 27.9 ton CO_2 eq. per ha per year for Malaysia is the highest of all, along with the annual LUC emissions of Indonesia (26.9 ton CO_2 eq. per ha). It is clear that cultivation of palm oil with equally high yields in areas with less tropical forest as natural vegetation can lead to a direct reduction of emissions. In these cases the total CCI of PFAD production and the resulting ketone bio-wax can be significantly reduced (>50%). This also clearly indicates

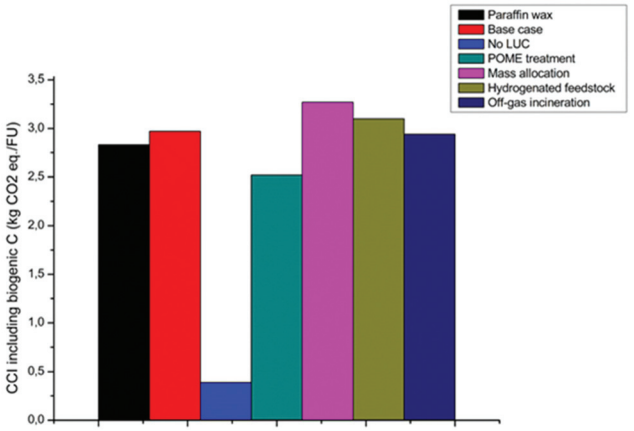

Fig. 7 Comparison of the impact on climate change (kg CO_2 eq. per FU) of PFAD bio-wax for different scenarios.

that, depending on the specific biomass feedstock choice for ketonization, critical selection of the right life cycle inventory data is essential to perform a reliable LCA.

The second scenario is related to the biogenic methane emissions during anaerobic open pond POME treatment (0.47 kg CO_2 eq. per FU), as introduced at the beginning of this section. Incorporation of a POME treatment step that utilizes anaerobic digestion in a closed system is a new and recent trend in the palm oil industry to reduce greenhouse gas emissions and other environmental burdens. Its benefits go beyond the mere reduction of biogenic methane emissions and the associated climate change impact.[90,91] It avoids local environmental burdens associated with POME discharge for example, while the produced biogas can be used as a renewable energy source. For this scenario, the biogenic methane emissions have been tracked and used for thermal energy production from the captured biogas (description in ESI†). For this scenario, the CCI impact of PFAD bio-wax is reduced from 2.94 to 2.50 kg CO_2 eq. per FU, which is a 15% reduction and 12% lower than the CCI of fossil paraffin wax. Controlled treatment of POME is advised due to its potential to develop a more sustainable feedstock, and as a direct consequence more environmentally friendly bio-waxes.

Thirdly, a mass allocation scenario was included based on the mass flows of the crude palm oil refining process. This allocation method is often used in LCA studies and distributes the environmental impact among products solely on a mass basis, without taking their economic values into consideration. The mass allocation factor of PFAD is 4.5%, which results in a scenario with a CCI of PFAD bio-wax of 3.23 kg CO_2 eq. per FU, which is 9.8% higher than in the case of economic allocation (Fig. 7).

As discussed in section 3.3, hydrogenation of PFAD can be performed prior to ketonization when the target application requires a bio-wax with very high saturated ketone content (up to 96%). While it has already been reported that the climate change impact of hydrogenation is very low during saturated fatty acid production,[81] this scenario was included in our analysis. Taking into account the climate change impacts of the hydrogenation conditions (thermal energy), H_2 and hydrogenation catalyst, a total CCI value of 3.10 kg CO_2 eq. per FU was calculated for the hydrogenated PFAD wax (ESI, Table S7†). As such, the presented process also allows flexibility depending on the desired final product, with only a minimal (5%) increase of the total global warming potential (without considering hydrogenation economics).

A scenario including off-gas incineration was considered due to the presence of (trace amounts of) methane, which is approximately 25 times more potent as GHG over 100 years than CO_2. The difference in CCI between off-gas emission and incineration is only 0.003 kg CO_2 eq. per FU, which is 0.1% of the total impact. In this case, there is no potential for further emission reduction since the absolute amount of methane in the off-gas is very so low.

To conclude this section, the difference in product lifetimes of the paraffin and bio-waxes can also be considered. As shown in section 3.4, the ketone bio-waxes have the potential to replace the current fossil benchmarks in hydrophobization applications. While the chemical structures of the long-chain ketones and alkanes are very similar, the presence of C=O (and C=C and COOH in case of unsaturated ketonization substrates) could lead to a scenario with a difference in wax lifetime between both products, depending on the target application. This is presented in Fig. S23,† where the CCI of bio-wax was calculated for bio-wax lifetimes ranging between 10–200% compared to the lifetime of paraffin wax. The respective carbon footprint values range between 29.4–1.47 kg CO_2 eq. per FU, showing the importance of sufficient bio-wax lifetime to obtain a competitive CCI value. Regarding the latter, we have already shown the desirable thermal stability of the PFAD bio-wax under oxidative conditions, which was similar to that of commercial paraffin wax for hydrophobization purposes. On the topic of biodegradability and the negative effect of product littering on the environment, the presence of chemical functionalities in the ketone bio-waxes can be advantageous compared to the current fossil benchmarks due to faster and more complete degradation although the information on these topics is still rather scarce. For instance, according to the European Chemicals Agency (ECHA) database, the stearone ketone is classified as not readily biodegradable in water (39–46% degradation in 28 days), but with low potential for bioaccumulation in organisms.[92] For the fatty acid dimer side products, no bioaccumulation risk is observed, while they are classified as not rapidly biodegradable (<10% in 28 days).[93] In comparison, the ECHA database cites 31% degradation of paraffin waxes in water after 28 days.[94] Others have found half-life values of 2–12 days for C_{10}–C_{36} alkanes in seawater.[95] Various studies have shown that the biodegradation rates of hydrocarbons may vary significantly depending on composition, test methodology and environmental conditions.[96,97] For both the ketone and paraffin waxes, prediction of biodegradability or bioaccumulation based on chemical composition is even more complex due to the heterogeneous nature

of the mixtures. In future research, both long term application testing as well as biodegradability studies could shed new light on these topics for the ketone bio-waxes. However, based on the thermal stability tests, molecular structures and current literature, it is reasonable to assume satisfactory stability and biodegradability characteristics for the bio-waxes in relationship to the current paraffin benchmarks.

Carbon footprint of ketone bio-waxes originating from other fatty acid feedstock. While this study has mainly focussed on the ketonization of PFAD, other fatty acids can also be converted with high product yields of waxy ketones (Table 5 and Table S1†). Because feedstock is one of the major hotspots of the PFAD bio-wax life cycle, the aim of this paragraph is to assess the potential CCI of ketone bio-waxes originating from other commercially available fats and oils. For this purpose, literature data is used. It is evident from our results that the scope, goal, definition and methodology will determine the absolute LCA outcome. As such the largest challenge lies in the availability of literature that uses a similar methodology for the impact of oil and fat production.

A LCA study was published on five commercial plant oils that rank in the global top six of largest vegetable oil production volumes, being palm, soybean, rapeseed, sunflower and peanut oil.[98] Here, LUC emissions were included while a consequential rather than attributional model was applied. Regarding the CCI (including biogenic carbon) values of the feedstock, the author found 2.02, 2.02, 0.26, 0.76 and 4.72 kg CO_2 eq. per kg refined oil for palm, soybean, rapeseed, sunflower and peanut, respectively. In another recent study, life cycle inventory data of bio-based surfactants and their biomass precursors were published, which included refined palm kernel oil (3.27 kg CO_2 eq. per kg), refined coconut oil (−1.94 kg CO_2 eq. per kg) and beef tallow (−1.53 kg CO_2 eq. per kg).[99] These data were used to calculate predicted CCI values of their respective ketone bio-waxes synthesized by our process (description in ESI†). A "theoretical" fatty acid waste stream was also incorporated into our results, for which the CCI of the cultivation or pre-ketonization stage is set to zero. This approach is based on the guidelines of the International Reference Life Cycle Data System (ILCD) by the Joint Research Centre (JRC) of the European Commission.[100] For waste materials (negative market value), the impact of the first life cycle and following treatments should not be included into the second life cycle up to the point where a positive market value is generated. These waste streams can include any vegetable or animal based products which have no or limited application for the production of chemicals. Some examples which may be interesting for future ketonization purposes include used cooking oils, non-food fatty acid side streams and (category 1 and 2) residual animal fats.[101]

As shown in Fig. 8, the predicted CCI values (including biogenic carbon) of the bio-waxes vary between −0.07 and 7.26 kg CO_2 eq. per FU. In this case, bio-waxes originating from refined rapeseed and coconut oil, as well as from waste streams and beef tallow have a lower CCI than paraffin wax (2.83 kg CO_2 eq. per FU). While we have shown in this work that the CCI of PFAD bio-wax can be reduced significantly, the base case scenario was used for comparison here. In an ideal scenario, biomass substrates are chosen which are net carbon sinks and thus have a negative CCI value for the cultivation/pre-ketonization stage. Both our work and that of others[99] have shown that this heavily depends on the absence or pres-

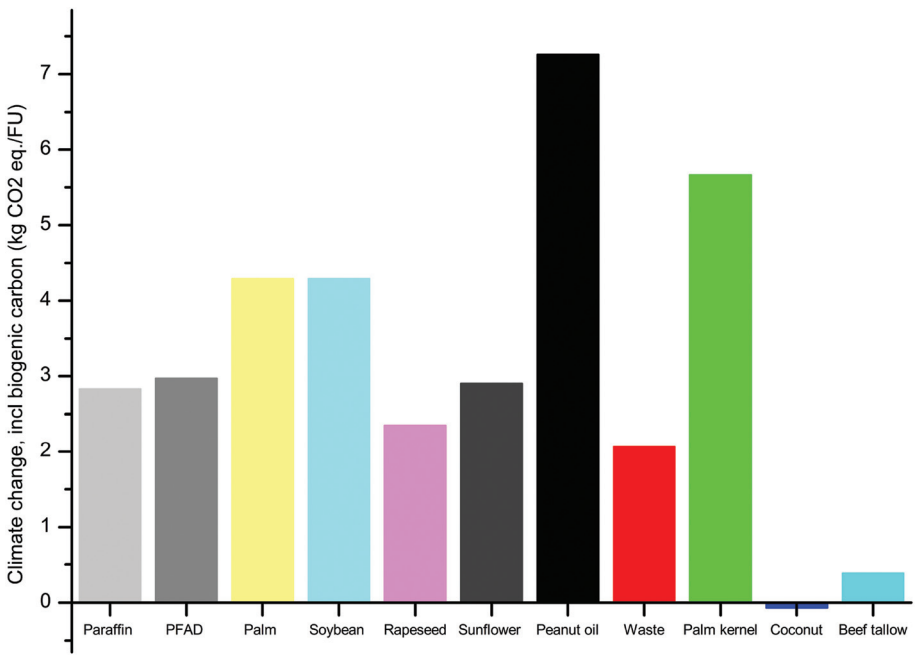

Fig. 8 Prediction of CCI (including biogenic C) of bio-waxes obtained by ketonization of vegetable oils and animal fats.[90,91]

ence of LUC emissions for vegetable oils, evidenced again by the coconut oil literature example here. If such a feedstock choice is not possible, the use of waste streams (zero impact) can significantly reduce the carbon emissions of bio-wax ketones (up to at least 27% lower than that of fossil paraffin wax).

4. Conclusion

In this first-of-its-kind study, we have shown the solvent-less liquid phase ketonization of commercial biomass fatty acids to C_{23}–C_{35} ketones with a high surface area Lewis acid TiO_2 catalyst. Due to the high activation energy and endothermic reaction enthalpy, full substrate conversion requires temperatures around 350 °C. Continuous removal of CO_2 and H_2O by-products from the reaction medium has a substantial positive effect on the conversion rate. With no treatment, the catalyst can only be partially reused due to loss of activity that is attributed to the loss of active surface area, coke formation and sintering of the active material. The degree of substrate unsaturation has a significant impact on the reaction selectivity, with the presence of oleic and linoleic acids also driving the formation of fatty acid dimer side products, but this had no adverse effect on the bio-wax wood hydrophobization property. Prior hydrogenation of the unsaturated feedstock was shown to result in saturated bio-waxes with very high ketone content (>95%), which is of use when higher purities are required.

Based on the lab scale ketonization results, an integrated process scheme was designed for ketone bio-wax production from fatty acid feedstock. This design includes mass and energy balances for all relevant steps and starts from substrate unloading to final product storage. Due to full utilization of the starting material and final solid bio-wax product, only TiO_2 catalyst and N_2 are necessary additional mass inputs. From the total energy balance, it can be concluded that the ketonization reaction is the most energy intensive step, while heat integration and recycling can significantly reduce the net energy demand of the entire process. The ketone bio-wax originating from palm fatty acid distillate was tested as hydrophobization agent for wood composite materials in an aqueous wax emulsion application. Compared to previously synthesized ketone bio-waxes and the current benchmark fossil paraffin waxes, similar or better water repellence properties were achieved. Furthermore, TGA analysis showed its good thermal stability, showing potential to replace the current fossil based standards in this kind of application.

Next, a combined Green Chemistry and LCA study was carried out to evaluate the environmental impact of the PFAD bio-wax life cycle, showing that the ketonization of long-chain fatty acids exhibits excellent atom economy and carbon efficiency values. This led us to further perform a detailed comparative cradle-to-grave life cycle assessment to determine the broader environmental impact of the bio-wax product. A hotspot and sensitivity analysis identified and evaluated three hotspots for the ketone bio-wax life cycle: substrate cultivation, catalyst production and end-of-life wax incineration. These aspects are to be prioritized when targeting an overall impact reduction of the entire cradle-to-grave life cycle.

Different scenarios were analysed for PFAD based bio-wax, which show the sometimes dramatic impact of multiple aspects of the agricultural process (geographical location of cultivation, land use change emissions, waste treatment, production efficiency, use of fertilizers, *etc.*) on the overall impact results. Specifically for PFAD based bio-wax, the CCI values vary between 0.39–3.23 kg CO_2 eq. per FU, which equates to a 87% reduction up to a 16% increase compared to the CCI of fossil paraffin wax (2.83 kg CO_2 eq. per FU). Both hydrogenation pretreatment and off-gas incineration scenarios showed no significant impact on the total CCI of bio-wax. Furthermore, the CCI of other commercial fatty acid feedstock, ranging from −0.07 to 7.26 kg CO_2 eq. per FU, were calculated based on analysis of available literature data. Valorisation of suitable vegetable oils and animal fats *via* ketonization may significantly reduce the carbon footprint compared to paraffin wax, whereas careless selection may yield substantial CCI increases. Ideally, biomass substrates (including waste streams) with negative CCI values for the pre-ketonization stage are chosen.

Finally, further catalytic research into improving the ketonization reaction rate and TiO_2 catalyst reusability may yield significant improvements in reducing multiple environmental impacts. Regarding catalyst synthesis, manufacturers should aim on reducing the energy requirement, using more renewable energy sources and more efficient use and recycling of high impact reagents such as sulphuric acid.

Conflicts of interest

B. S., B. B., J. C. and C. V. C. are authors on a patent application cited in this work, filed by Govi NV (EP3450517A1). All other authors declare that they have no competing interests.

Acknowledgements

B. B. acknowledges the Research Foundation-Flanders (FWO) for a PhD Fellowship (strategic basic research – SB). B. S. acknowledges VLAIO for the Catalisti FISCH-ICON Biowax Project. We thank Fermin Zarza and Paul Devuyst at Exyte for contributing to the development of the integrated industrial process scheme. We thank Govi NV for performing the application tests.

Notes and references

1 R. A. Sheldon, Green and sustainable manufacture of chemicals from biomass: state of the art, *Green Chem.*, 2014, **16**(3), 950–963.

2 P. Gallezot, Conversion of biomass to selected chemical products, *Chem. Soc. Rev.*, 2012, **41**(4), 1538–1558.

3 G. A. Mansoori, H. L. Barnes and G. M. Webster, in *Chapter 4 | Petroleum Waxes*, ed. G. Totten, R. Shah and D. Forester, ASTM International, West Conshohocken, PA, 2019, pp. 79–113.

4 C. Leray, Waxes, in *Kirk–Othmer Encyclopedia of Chemical Technology*, 2006.

5 MarketsandMarkets, Industrial Wax Market by Type (Fossil based, Synthetic based, Bio based), Application (Candles, Packaging, Coatings & Polishes, Hot-melt Adhesives, Tires & Rubber, *Cosmetics & Personal Care, Food), and Region – Global Forecast to*, 2026, https://www.marketsandmarkets.com/Market-Reports/industrial-wax-market-97935975.html?gclid=CjwKCAjwkPX0BRBKEiwA7THxiEp4IEmxj7z5X316ewtzOwT9REPVuYPlKYcMubKGv-QdN6dPDMDl1BoC5bYQAvD_BwE, (accessed August 2020).

6 Grand View Research, Paraffin Wax Market Size, *Share & Trends Analysis Report By Application (Candles, Packaging, Cosmetics, Hotmelts, Board Sizing, Rubber), By Region, And Segment Forecasts, 2018–2025*, https://www.grandviewresearch.com/industry-analysis/paraffin-wax-market, (accessed August 2020).

7 M. Balakrishnan, G. E. Arab, O. B. Kunbargi, A. A. Gokhale, A. M. Grippo, F. D. Toste and A. T. Bell, Production of renewable lubricants via self-condensation of methyl ketones, *Green Chem.*, 2016, **18**(12), 3577–3581.

8 S. Liu, T. R. Josephson, A. Athaley, Q. P. Chen, A. Norton, M. Ierapetritou, J. I. Siepmann, B. Saha and D. G. Vlachos, Renewable lubricants with tailored molecular architecture, *Sci. Adv.*, 2019, **5**(2), eaav5487.

9 J. G. Speight, 7 - Synthetic liquid fuel production from gasification, in *Gasification for Synthetic Fuel Production*, ed. R. Luque and J. G. Speight, Woodhead Publishing, 2015, pp. 147–174.

10 M. E. Dry, The Fischer–Tropsch process: 1950–2000, *Catal. Today*, 2002, **71**(3), 227–241.

11 B. Boekaerts and B. F. Sels, Catalytic advancements in carboxylic acid ketonization and its perspectives on biomass valorisation, *Appl. Catal., B*, 2021, **283**, 119607.

12 R. Kumar, N. Enjamuri, S. Shah, A. S. Al-Fatesh, J. J. Bravo-Suárez and B. Chowdhury, Ketonization of oxygenated hydrocarbons on metal oxide based catalysts, *Catal. Today*, 2018, **302**, 16–49.

13 E. R. Squibb, Improvement in the manufacture of acetone 1, *J. Am. Chem. Soc.*, 1895, **17**(3), 187–201.

14 T. N. Pham, T. Sooknoi, S. P. Crossley and D. E. Resasco, Ketonization of Carboxylic Acids: Mechanisms, Catalysts, and Implications for Biomass Conversion, *ACS Catal.*, 2013, **3**(11), 2456–2473.

15 A. V. Ignatchenko, Multiscale approach for the optimization of ketones production from carboxylic acids by the decarboxylative ketonization reaction, *Catal. Today*, 2019, **338**, 3–17.

16 M. Renz, Ketonization of Carboxylic Acids by Decarboxylation: Mechanism and Scope, *Eur. J. Org. Chem.*, 2005, **2005**(6), 979–988.

17 A. E. King, T. J. Brooks, Y.-H. Tian, E. R. Batista and A. D. Sutton, Understanding Ketone Hydrodeoxygenation for the Production of Fuels and Feedstocks From Biomass, *ACS Catal.*, 2015, **5**(2), 1223–1226.

18 H. M. Wang, J. Male and Y. Wang, Recent Advances in Hydrotreating of Pyrolysis Bio-Oil and Its Oxygen-Containing Model Compounds, *ACS Catal.*, 2013, **3**(5), 1047–1070.

19 P. N. R. Vennestrøm, C. M. Osmundsen, C. H. Christensen and E. Taarning, Beyond Petrochemicals: The Renewable Chemicals Industry, *Angew. Chem., Int. Ed.*, 2011, **50**(45), 10502–10509.

20 J. F. S. J. Alonso, I. G. Arribas and S. A. Miñambre, Study of combustion in residential oil burning equipment of animal by-products and derived products not intended for human consumption, *Int. J. Energy Environ. Eng.*, 2013, **4**(1), 31.

21 M. R. Teixeira, R. Nogueira and L. M. Nunes, Quantitative assessment of the valorisation of used cooking oils in 23 countries, *Waste Manage.*, 2018, **78**, 611–620.

22 A. Corma, M. Renz and C. Schaverien, Coupling Fatty Acids by Ketonic Decarboxylation Using Solid Catalysts for the Direct Production of Diesel, Lubricants, and Chemicals, *ChemSusChem*, 2008, **1**(8–9), 739–741.

23 K. Lee, M. Y. Kim and M. Choi, Effects of Fatty Acid Structures on Ketonization Selectivity and Catalyst Deactivation, *ACS Sustainable Chem. Eng.*, 2018, **6**(10), 13035–13044.

24 M. A. Jackson and S. C. Cermak, Cross ketonization of Cuphea sp. oil with acetic acid over a composite oxide of Fe, Ce, and Al, *Appl. Catal., A*, 2012, **431–432**, 157–163.

25 T. K. Phung, A. A. Casazza, P. Perego, P. Capranica and G. Busca, Catalytic pyrolysis of vegetable oils to biofuels: Catalyst functionalities and the role of ketonization on the oxygenate paths, *Fuel Process. Technol.*, 2015, **140**, 119–124.

26 B. Oliver-Tomas, M. Renz and A. Corma, High Quality Biowaxes from Fatty Acids and Fatty Esters: Catalyst and Reaction Mechanism for Accompanying Reactions, *Ind. Eng. Chem. Res.*, 2017, **56**(45), 12870–12877.

27 O. Back and P. Marion, Process For The Catalytic Decarboxylative Cross-ketonization Of Aryl And Aliphatic Carboxylic Acid, WO2018/229285A1, 2018/06/15, 2018.

28 J. Myllyoja, J. Jakkula, P. Aalto, E. Koivusalmi, J.-F. Selin and J. Moilanen, Process For Producing A Hydrocarbon Component, US2007/0161832A1, 2006/12/11, 2007.

29 E. Koivusalmi, I. Kilpelaeinen, P. Karhunen and J. Matikainen, Process For Producing A Branched Hydrocarbon Base Oil From A Feedstock Containing Aldehyde And/or Ketone, US7850841B2, 2006/12/12, 2010.

30 I. Hommeltoft Sven, Ketonization Process Using Oxidative Catalyst Regeneration, US9314785B1, 2014/11/13, 2016.

31 M. Kettunen, J. Myllyoja, R. Piilola, G. Sandström and P. Aalto, Simultaneous Production Of Base Oil And Fuel Components From Renewable Feedstock, EP2809745A1, 2012/11/01, 2014.

32 M. Kettunen, J. Myllyoja, R. Piilola, G. Sandstrom and P. Aalto, Dual Catalyst System For Performing A Ketonisation Reaction And A Hydrotreatment Reaction Simultaneously, US9545621B2, 2015/05/20, 2017.

33 J. Myllyoja, S. Kouva, J. Kohonen, R. Piilola, M. Kettunen, J. Makkonen and M. Hovi, Tio2 Catalyst In Ketonisation Reactions To Produce Rbo, WO2018/234186A1, 2018/06/15, 2018.

34 J. Kanervo, S. Toppinen and P. Nurmi, Method For Producing Ketones For Fuel And Oil Applications, US2019/0185759A1, 2018/12/17, 2019.

35 O. Back, R. Leroy and P. Marion, Process For The Decarboxylative Ketonization Of Fatty Acids Or Fatty Acid Derivatives, US10035746B2, 2016/05/04, 2018.

36 O. Back, R. Leroy and P. Marion, Processes For The Manufacture Of Secondary Fatty Alcohols, Internal Olefins And Internal Olefin Sulfonates, WO2019/161896A1, 2018/02/21, 2019.

37 W. Liu, Q. Zhu, X. Zhou and C. Peng, Comparative analyses of different biogenic CO_2 emission accounting systems in life cycle assessment, *Sci. Total Environ.*, 2019, **652**, 1456–1462.

38 W. Liu, Z. Yu, X. Xie, K. von Gadow and C. Peng, A critical analysis of the carbon neutrality assumption in life cycle assessment of forest bioenergy systems, *Environ. Rev.*, 2017, **26**(1), 93–101.

39 E. I. Wiloso, R. Heijungs, G. Huppes and K. Fang, Effect of biogenic carbon inventory on the life cycle assessment of bioenergy: challenges to the neutrality assumption, *J. Cleaner Prod.*, 2016, **125**, 78–85.

40 D. N. Vienescu, J. Wang, A. Le Gresley and J. D. Nixon, A life cycle assessment of options for producing synthetic fuel via pyrolysis, *Bioresour. Technol.*, 2018, **249**, 626–634.

41 T. Pham, D. Shi, T. Sooknoi and D. Resasco, Aqueous-phase ketonization of acetic acid over Ru/TiO2/carbon Catalysts, *J. Catal.*, 2012, **295**, 169–178.

42 G. Pacchioni, Ketonization of Carboxylic Acids in Biomass Conversion over TiO2 and ZrO2 Surfaces: A DFT Perspective, *ACS Catal.*, 2014, **4**(9), 2874–2888.

43 M. Tamura, K.-I. Shimizu and A. Satsuma, Comprehensive IR study on acid/base properties of metal oxides, *Appl. Catal., A*, 2012, **433–434**, 135–145.

44 J. Cocquyt, C. Van Caneyt, B. Boekaerts and B. Sels, Wood Composite Objects, EP3450517A1, 2018/08/28, 2019.

45 P. T. Anastas and J. C. Warner, *Green Chemistry: Theory and Practice*, Oxford University Press, 1998.

46 ISO, *International Standard ISO 14040 Environmental management—Life cycle assessment—Requirements and guidelines Management*, 2006.

47 ISO, *International Standard ISO 14044 Environmental management—Life cycle assessment—Requirements and guidelines Management*, 2006.

48 M. Z. Hauschild, R. K. Rosenbaum and S. I. Olsen, *Life cycle assessment*, Springer, 2018.

49 M. A. J. Huijbregts, Z. J. N. Steinmann, P. M. F. Elshout, G. Stam, F. Verones, M. Vieira, M. Zijp, A. Hollander and R. van Zelm, ReCiPe2016: a harmonised life cycle impact assessment method at midpoint and endpoint level, *Int. J. Life Cycle Assess.*, 2017, **22**(2), 138–147.

50 Thinkstep, "Process data set: Wax/Paraffins at refinery; from crude oil; production mix, at refinery; 38 MJ/kg net calorific value (en)". 2018.

51 Thinkstep, "Process data set: Palm oil, refined (incl. LUC as fossil CO_2); technology mix; production mix, at plant; refined (en)". 2018.

52 S. Wang and E. Iglesia, Experimental and Theoretical Evidence for the Reactivity of Bound Intermediates in Ketonization of Carboxylic Acids and Consequences of Acid–Base Properties of Oxide Catalysts, *J. Phys. Chem. C*, 2017, **121**(33), 18030–18046.

53 S. Shylesh, L. A. Bettinson, A. Aljahri, M. Head-Gordon and A. T. Bell, Experimental and Computational Studies of Carbon–Carbon Bond Formation via Ketonization and Aldol Condensation over Site-Isolated Zirconium Catalysts, *ACS Catal.*, 2020, **10**(8), 4566–4579.

54 T. Bezrodna, G. Puchkovska, V. Shymanovska, I. Chashechnikova, T. Khalyavka and J. Baran, Pyridine-TiO2 surface interaction as a probe for surface active centers analysis, *Appl. Surf. Sci.*, 2003, **214**, 222–231.

55 H.-Y. T. Chen, S. Tosoni and G. Pacchioni, A DFT study of the acid–base properties of anatase TiO2 and tetragonal ZrO2 by adsorption of CO and CO_2 probe molecules, *Surf. Sci.*, 2016, **652**, 163–171.

56 G. Martra, Lewis acid and base sites at the surface of microcrystalline TiO2 anatase: relationships between surface morphology and chemical behaviour, *Appl. Catal., A*, 2000, **200**(1), 275–285.

57 T. N. Pham, D. Shi and D. E. Resasco, Reaction kinetics and mechanism of ketonization of aliphatic carboxylic acids with different carbon chain lengths over Ru/TiO2 catalyst, *J. Catal.*, 2014, **314**, 149–158.

58 T. N. Pham, D. Shi and D. E. Resasco, Kinetics and Mechanism of Ketonization of Acetic Acid on Ru/TiO2 Catalyst, *Top. Catal.*, 2014, **57**(6), 706–714.

59 A. V. Ignatchenko and A. J. Cohen, Reversibility of the catalytic ketonization of carboxylic acids and of beta-keto acids decarboxylation, *Catal. Commun.*, 2018, **111**, 104–107.

60 A. V. Ignatchenko, T. J. DiProspero, H. Patel and J. R. LaPenna, Equilibrium in the Catalytic Condensation of Carboxylic Acids with Methyl Ketones to 1,3-Diketones and the Origin of the Reketonization Effect, *ACS Omega*, 2019, **4**(6), 11032–11043.

61 D. Y. Murzin, A. Bernas, J. Wärnå, J. Myllyoja and T. Salmi, Ketonization kinetics of stearic acid, *React. Kinet., Mech. Catal.*, 2019, **126**(2), 601–610.

62 S. Wang and E. Iglesia, Experimental and theoretical assessment of the mechanism and site requirements for ketonization of carboxylic acids on oxides, *J. Catal.*, 2017, **345**, 183–206.

63 C. A. Gaertner, J. C. Serrano-Ruiz, D. J. Braden and J. A. Dumesic, Ketonization Reactions of Carboxylic Acids

and Esters over Ceria–Zirconia as Biomass-Upgrading Processes, *Ind. Eng. Chem. Res.*, 2010, **49**(13), 6027–6033.
64 M. Gliński and J. Kijeński, Catalytic Ketonization of Carboxylic Acids Synthesis of Saturated and Unsaturated Ketones, *React. Kinet. Catal. Lett.*, 2000, **69**(1), 123–128.
65 J. Zhang, A. Nuñez, G. D. Strahan, R. Ashby, K. Huang, R. A. Moreau, Z. Yan, L. Chen and H. Ngo, An advanced process for producing structurally selective dimer acids to meet new industrial uses, *Ind. Crops Prod.*, 2020, **146**, 112132.
66 K. J. Park, M. Kim, S. Seok, Y.-W. Kim and D. H. Kim, Quantitative analysis of cyclic dimer fatty acid content in the dimerization product by proton NMR spectroscopy, *Spectrochim. Acta, Part A*, 2015, **149**, 402–407.
67 F. Piccinno, R. Hischier, S. Seeger and C. Som, From laboratory to industrial scale: a scale-up framework for chemical processes in life cycle assessment studies, *J. Cleaner Prod.*, 2016, **135**, 1085–1097.
68 D. J. Anneken, S. Both, R. Christoph, G. Fieg, U. Steinberner and A. Westfechtel, Fatty Acids, in *Ullmann's Encyclopedia of Industrial Chemistry*, 2006.
69 R. M. Stephenson and S. Malanowski, *Handbook of the Thermodynamics of Organic Compounds*, 1987.
70 R. G. Jenkins, Chapter 16 - Thermal Gasification of Biomass – A Primer, in *Bioenergy*, ed. A. Dahiya, Academic Press, Boston, 2015, pp. 261–286.
71 F. O. Cedeño, M. M. Prieto and J. Xiberta, Measurements and Estimate of Heat Capacity for Some Pure Fatty Acids and Their Binary and Ternary Mixtures, *J. Chem. Eng. Data*, 2000, **45**(1), 64–69.
72 K. Nakasone, K. Takamizawa, K. Shiokawa and Y. Urabe, Simultaneous determination of the heat capacity and the heat of the transitions for long-chain compounds with a heat-flux type DSC, *Thermochim. Acta*, 1994, **233**(2), 175–185.
73 M. Tschulkow, T. Compernolle, S. Van Den Bosch, J. Van Aelst, I. Storms, M. Van Dael, G. Van Den Bossche, B. Sels and S. Van Passel, Integrated techno-economic assessment of a biorefinery process: The high-end valorization of the lignocellulosic fraction in wood streams, *J. Cleaner Prod.*, 2020, **266**, 122022.
74 Y. Liao, S.-F. Koelewijn, G. Van den Bossche, J. Van Aelst, S. Van den Bosch, T. Renders, K. Navare, T. NicolaΓÏ, K. Van Aelst, M. Maesen, H. Matsushima, J. M. Thevelein, K. Van Acker, B. Lagrain, D. Verboekend and B. F. Sels, A sustainable wood biorefinery for lower carbon footprint chemicals production, *Science*, 2020, **367**(6484), 1385–1390.
75 Malaysian Palm Oil Board, Prices of selected oils and fats (North-West Europe Market US$/Tonne) – 2020, http://bepi.mpob.gov.my/index.php/en/?option=com_content&view=article&id=906&Itemid=138 (accessed September 2020).
76 The World Bank, *World Bank Commodities Price Data*, http://pubdocs.worldbank.org/en/520721601663433090/CMO-Pink-Sheet-October-2020.pdf (accessed August 2020).
77 Eurostat, Gas prices for non-household consumers – bi-annual data (from 2007 onwards), https://ec.europa.eu/eurostat/databrowser/view/nrg_pc_203/default/table?lang=en, (accessed September 2020).
78 R. A. Sheldon, The E Factor: fifteen years on, *Green Chem.*, 2007, **9**(12), 1273–1283.
79 P. T. Anastas and J. B. Zimmerman, Chapter 2 The twelve principles of green engineering as a foundation for sustainability, in *Sustainability Science and Engineering*, ed. M. A. Abraham, Elsevier, 2006, vol. 1, pp. 11–32.
80 D. P. Fogliatti, S. A. Kemppainen, T. N. Kalnes, J. Fan and D. R. Shonnard, Life Cycle Carbon Footprint of Linear Alkylbenzenesulfonate from Coconut Oil, Palm Kernel Oil, and Petroleum-Based Paraffins, *ACS Sustainable Chem. Eng.*, 2014, **2**(7), 1828–1834.
81 L. M. Tufvesson and P. Börjesson, Wax production from renewable feedstock using biocatalysts instead of fossil feedstock and conventional methods, *Int. J. Life Cycle Assess.*, 2008, **13**(4), 328.
82 P. Khatri and S. Jain, Environmental life cycle assessment of edible oils: A review of current knowledge and future research challenges, *J. Cleaner Prod.*, 2017, **152**, 63–76.
83 II. Manufacture of Paraffin Waxes and Ceresins from Petroleum, in *Developments in Petroleum Science*, ed. M. Freund, R. Csikós, S. Keszthelyi and G. Y. Mózes, Elsevier, 1982, vol. 14, pp. 141–239.
84 J. G. Speight, Chapter 3 - Hydrocarbons from Petroleum, in *Handbook of Industrial Hydrocarbon Processes*, ed. J. G. Speight, Gulf Professional Publishing, Boston, 2011, pp. 85–126.
85 N. Z. Abdul Kapor, G. P. Maniam, M. H. A. Rahim and M. M. Yusoff, Palm fatty acid distillate as a potential source for biodiesel production-a review, *J. Cleaner Prod.*, 2017, **143**, 1–9.
86 A. Meijide, C. de la Rua, T. Guillaume, A. Röll, E. Hassler, C. Stiegler, A. Tjoa, T. June, M. D. Corre, E. Veldkamp and A. Knohl, Measured greenhouse gas budgets challenge emission savings from palm-oil biodiesel, *Nat. Commun.*, 2020, **11**(1), 1089.
87 J. C. Quezada, A. Etter, J. Ghazoul, A. Buttler and T. Guillaume, Carbon neutral expansion of oil palm plantations in the Neotropics, *Sci. Adv.*, 2019, **5**(11), eaaw4418.
88 G. Time and S. Isic, *Ecoinvent 3.3 dataset documentation on titanium dioxide production, sulfate process for Europe*, 2005.
89 H. C. Flynn, L. M. I. Canals, E. Keller, H. King, S. Sim, A. Hastings, S. Wang and P. Smith, Quantifying global greenhouse gas emissions from land-use change for crop production, *Glob. Change Biol.*, 2012, **18**(5), 1622–1635.
90 M. J. Chin, P. E. Poh, B. T. Tey, E. S. Chan and K. L. Chin, Biogas from palm oil mill effluent (POME): Opportunities and challenges from Malaysia's perspective, *Renewable Sustainable Energy Rev.*, 2013, **26**, 717–726.

91 S. S. Harsono, P. Grundmann and S. Soebronto, Anaerobic treatment of palm oil mill effluents: potential contribution to net energy yield and reduction of greenhouse gas emissions from biodiesel production, *J. Cleaner Prod.*, 2014, **64**, 619–627.
92 ECHA, Pentatriacontan-18-one, https://echa.europa.eu/nl/registration-dossier/-/registered-dossier/27934/7/3/2 (accessed 29th of June 2021).
93 ECHA, Fatty acids, C18-unsatd., dimers, https://echa.europa.eu/nl/registration-dossier/-/registered-dossier/16133 (accessed 29th of June 2021).
94 ECHA, Paraffin waxes and Hydrocarbon waxes, https://echa.europa.eu/nl/registration-dossier/-/registered-dossier/15503 (accessed 29th of June 2021).
95 O. G. Brakstad, U. Farooq, D. Ribicic and R. Netzer, Dispersibility and biotransformation of oils with different properties in seawater, *Chemosphere*, 2018, **191**, 44–53.
96 D. M. Brown, L. Camenzuli, A. D. Redman, C. Hughes, N. Wang, E. Vaiopoulou, D. Saunders, A. Villalobos and S. Linington, Is the Arrhenius-correction of biodegradation rates, as recommended through REACH guidance, fit for environmentally relevant conditions? An example from petroleum biodegradation in environmental systems, *Sci. Total Environ.*, 2020, **732**, 139293.
97 J. Greskowiak, E. Hamann, V. Burke and G. Massmann, The uncertainty of biodegradation rate constants of emerging organic compounds in soil and groundwater – A compilation of literature values for 82 substances, *Water Res.*, 2017, **126**, 122–133.
98 J. H. Schmidt, Life cycle assessment of five vegetable oils, *J. Cleaner Prod.*, 2015, **87**, 130–138.
99 D. Schowanek, T. Borsboom-Patel, A. Bouvy, J. Colling, J. A. de Ferrer, D. Eggers, K. Groenke, T. Gruenenwald, J. Martinsson, P. McKeown, B. Miller, S. Moons, K. Niedermann, M. Pérez, C. Schneider and J.-F. Viot, New and updated life cycle inventories for surfactants used in European detergents: summary of the ERASM surfactant life cycle and ecofootprinting project, *Int. J. Life Cycle Assess.*, 2018, **23**(4), 867–886.
100 European Commission, Joint Research Centre and Institute for Environment and Sustainability, *International Reference Life Cycle Data System (ILCD) Handbook - General guide for Life Cycle Assessment: Provisions and Action Steps*, Publications Office of the European Union, Luxembourg, 1st edn, 2010.
101 F. Horst and M. Stefanie, *Analysis of allocation approaches of animal by-product treatment in the context of life cycle assessments*, Institut für Energieund Umweltforschung Heidelberg GmbH, 2014.